

Spatial and temporal variability and connectivity of the marine environment of the South Sandwich Islands, Southern Ocean

Sally E. Thorpe^{*}, Eugene J. Murphy

British Antarctic Survey, Natural Environment Research Council, High Cross, Madingley Road, Cambridge, CB3 0ET, UK

ARTICLE INFO

Keywords:

Antarctica
Scotia sea
Antarctic Circumpolar Current
Weddell Gyre
Sea ice
Phytoplankton
Marine ecology
Ecosystem function
Ecosystem management

ABSTRACT

The South Sandwich Islands form the eastern boundary to the highly biologically productive Scotia Sea in the southwest Atlantic sector of the Southern Ocean and are part of a large Marine Protected Area. The South Sandwich Islands have a complex marine environment that is influenced by both the Antarctic Circumpolar Current and the Weddell Gyre, and seasonal sea ice. Here we investigate the local and regional dynamics and variability of the ocean and sea ice to inform management of the region. Remotely sensed sea surface temperature (SST), sea ice concentration and chlorophyll *a* data from 2009 to 2021 are used to define the mean seasonal cycle in the environment and the associated temporal and spatial variability. While sea surface temperature and sea ice have a clearly defined seasonality, local chlorophyll blooms are irregular in timing, location and magnitude. Interannual variability in summer SST is strongly positively correlated along the island arc. The islands experience very different winter sea ice conditions from year to year, with marked variability in sea ice distribution and duration. Surface chlorophyll blooms develop in most years close to the island arc, but there is little spatial consistency and there are years where blooms are not observed. The timing and pattern of sea ice retreat appears to be a key driver in the formation of chlorophyll blooms, with their propagation affected by local circulation, but additional local processes are also important. Trajectories of near-surface satellite tracked surface buoys and Argo floats, together with an analysis of sea surface height output from a global reanalysis product, demonstrate the connectivity of the South Sandwich Islands to the wider regional marine system. Enhanced current flows around and between the South Sandwich Islands are likely to affect the transport and exchange of material along the island arc. The South Sandwich Islands are connected with the Scotia and Weddell seas, with contribution from the different regions varying according to latitude along the island arc. There are also connections with islands downstream including Bouvet, Crozet and Kerguelen Islands and seamounts, with possible return flow via the Weddell Gyre. Our analyses indicate that accounting for the complexity and variability in the South Sandwich Islands marine environment will be crucial in the development of conservation and fisheries management procedures.

1. Introduction

The South Sandwich Islands (SSI) are located in the southwest Atlantic sector of the Southern Ocean, approximately 700 km southeast of the island of South Georgia. The high biodiversity and biomass of the South Georgia and SSI region, together with its use by commercial fisheries, led to the establishment of a Marine Protected Area in 2012 (Handley et al., 2020; Rogers et al., 2015; Trathan et al., 2014). The inaccessibility of the SSI has made it difficult to carry out studies in this region, with relatively little information available to date on the marine environment or the structure and functioning of its ecosystem. However,

there is a current focus on improving the understanding of the marine system to contribute to informing the management of the islands and the Marine Protected Area (e.g., Hogg et al., 2021; Liszka et al., this issue). Here we use a range of datasets from remote sensing, autonomous instruments and reanalysis products to describe the spatial and temporal variability in the marine environment of the SSI from 2009 to 2021, to both complement field surveys that provide information at specific points in time (Liszka et al., this issue; Tynan et al., 2016; Ward et al., 2004) and to provide context for projected changes in Southern Ocean environments in the coming decades that are expected to affect the distributions of organisms and ecosystem structure and functioning

^{*} Corresponding author.

E-mail address: seth@bas.ac.uk (S.E. Thorpe).

<https://doi.org/10.1016/j.dsr2.2022.105057>

Received 25 August 2021; Received in revised form 24 February 2022; Accepted 5 March 2022

Available online 12 March 2022

0967-0645/© 2022 The Authors. Published by Elsevier Ltd. This is an open access article under the CC BY license (<http://creativecommons.org/licenses/by/4.0/>).

(Cavanagh et al., 2021).

The SSI are part of an active volcanic arc that forms the eastern boundary to the Scotia Sea (Fig. 1). The island group is located between $\sim 56^{\circ}\text{S}$ and 60°S and consists of 11 small islands and several seamounts (Leat et al., 2014). The islands are separated by passages of varying depths and widths. East of, and parallel to, the SSI arc is a deep (>8000 m) trench, a result of tectonic plate subduction. Bounded to the north and south by the North and South Scotia Ridges respectively, the Scotia Sea is an area of intense mesoscale activity, mixing and water mass transformation, and a major route for the export of deep waters formed near the Antarctic continent (e.g., Naveira Garabato et al., 2002). The circulation of the Scotia Sea is dominated by the eastward-flowing Antarctic Circumpolar Current (ACC) which is topographically steered northwards around the SSI before returning southwards east of the island arc (Orsi et al., 1995). This means that the SSI are situated south of the ACC, within subpolar waters influenced by the Weddell Gyre, a large cyclonic gyre mainly driven by wind forcing that extends from the Antarctic Peninsula in the west to $\sim 30^{\circ}\text{E}$ and possibly to 50°E (Deacon, 1979; Orsi et al., 1993; Park et al., 2001). The ACC and Weddell Gyre are separated in the Scotia Sea by the Weddell-Scotia Confluence (WSC), an area of mixing between the two hydrographic regimes with additional waters from the continental shelf of the Antarctic Peninsula (Whitworth et al., 1994). The southern boundary of the ACC (SB) separates the ACC from the subpolar waters to the south. The boundary between the WSC and the Weddell Gyre, referred to as the Weddell Front, follows a convoluted path aligned with the South Scotia Ridge (Heywood et al., 2004). The properties of the WSC become less distinct with distance from the Antarctic Peninsula but signals of the WSC have been observed to $\sim 22^{\circ}\text{E}$ (Brandon et al., 2004; Orsi et al., 1993).

Sea ice is another dominant feature of the marine environment of the SSI. The SSI lie within the seasonal sea ice zone (Fig. 1; Fetterer et al., 2017); sea ice extends across the island arc in winter in most years, before retreating far south of the islands in summer. The seasonal cycle

of sea ice is a key physical driver of ecosystem structure and dynamics in the Southern Ocean (Arrigo and Thomas, 2004; Constable et al., 2014; Ducklow et al., 2007; Saba et al., 2014; Smith et al., 2007; Thorpe et al., 2007) and there is strong interannual variability in both the timing of the advance and retreat of sea ice and its spatial distribution in the Scotia Sea and SSI region (Hart and Convey, 2018; Murphy et al., 2014). The sea ice cycle impacts the local ecosystem through modifying surface fluxes of heat and freshwater, and hence the stability of the near-surface water column, and availability of light and nutrients, which can lead to intense spring phytoplankton blooms as sea ice retreats (e.g., Froneman et al., 1995; Perissinotto et al., 1992; Tynan et al., 2016).

Large areas of the Southern Ocean are high nutrient-low chlorophyll regions, where phytoplankton bloom formation is largely limited by supply of iron (Boyd et al., 2010; de Baar et al., 1995). However, iron input into the Scotia Sea, predominantly from current interactions with sediment, makes it one of the most productive regions of the Southern Ocean (Borrione et al., 2014; Hodson et al., 2017). In coastal regions around the Antarctic Peninsula and to the northwest of South Georgia, extensive blooms occur in the same area in most years (Korb et al., 2008, 2012). Over much of the Scotia Sea and the northern Weddell Sea, however, the magnitude, timing and spatial distribution of blooms is highly variable (Borrione and Schlitzer, 2013; Nielsdottir et al., 2012; Park et al., 2010; Whitehouse et al., 2012) and adds to the complex dynamics of the regional ecosystem. Advection of the blooms downstream of the sites of formation by the regional current systems can enhance productivity further afield (Borrione et al., 2014; Hinz et al., 2012; Jiang et al., 2019; Sergi et al., 2020).

The seasonal production of the Scotia Sea supports a diverse biological community with elevated levels of biomass through the food chain (Atkinson et al., 2001; Murphy et al., 2007; Ward et al., 2004, 2012a, 2012b). The composition of zooplankton communities tends to be generally similar across the Scotia Sea, although the relative abundance of different groups and species varies (Ward et al., 2004, 2012b).

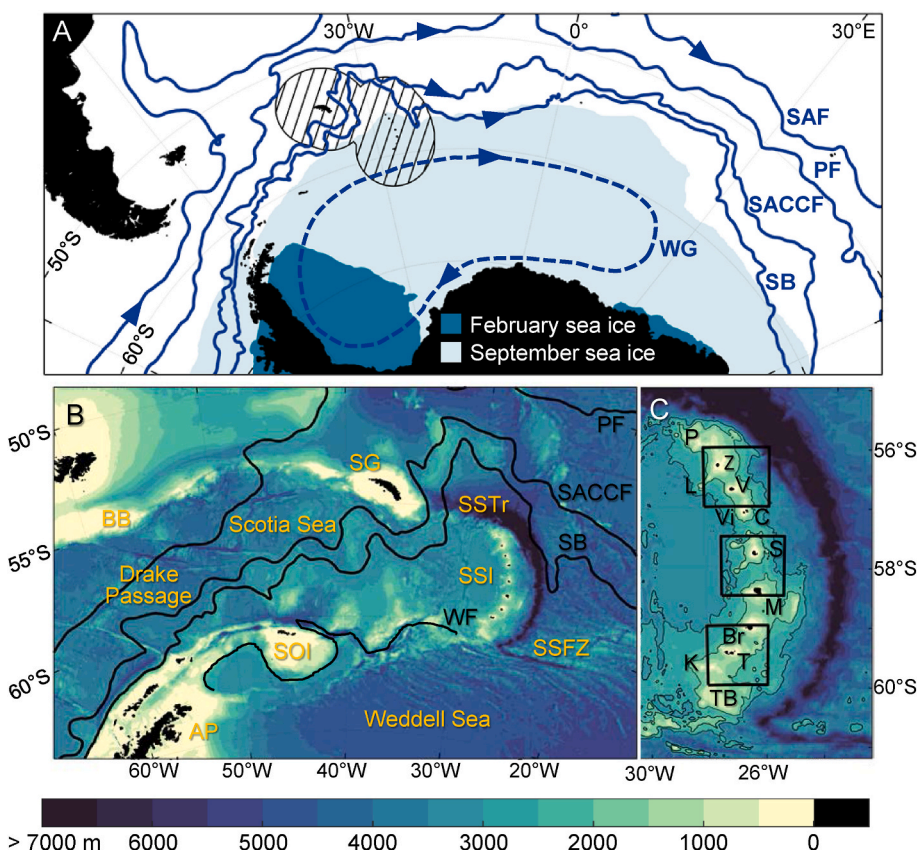


Fig. 1. Major oceanographic features and bathymetry of the Scotia Sea and the South Sandwich Island Arc. A) The Weddell Gyre (dashed blue line) and the mean location of the major fronts of the Antarctic Circumpolar Current (ACC; solid blue lines) comprising the Subantarctic Front (SAF), Polar Front (PF), Southern ACC Front (SACCF), and southern boundary of the ACC (SB) (Park and Durand, 2019; Park et al., 2019). Also shown is the median summer (February) and winter (September) sea ice extent for 1981–2010 (dark and light blue shading, respectively; Fetterer et al., 2017), and the South Georgia and South Sandwich Islands Marine Protected Area (hatched area). B) Bathymetry (m) of the Scotia Sea (GEBCO Compilation Group, 2020). Additional oceanographic features marked are the Weddell Front (WF; Heywood et al., 2004) and the Weddell-Scotia Confluence (WSC). Geographic and bathymetric features are labelled: Antarctic Peninsula (AP), Burdwood Bank (BB), South Georgia (SG), South Orkney Islands (SOI), South Sandwich Islands (SSI), South Sandwich Fracture Zone (SSFZ), and South Sandwich Trench (SSTr). C) Islands (I) and bathymetric features of the South Sandwich Island Arc: Protector Shoal (P), Zavadvoski I. (Z), Leskov I. (L), Visokoi I. (V), Candelmas I. (C), Vindication I. (Vi), Saunders I. (S), Montagu I. (M), Bristol I. (Br), Southern Thule (T) comprising Bellingshausen, Thule and Cook islands, Kemp seamounts (K) and Tyrell Bank (TB). The 2000 m and 3000 m isobaths are marked (thin black line). Three study regions used for analyses are shown (thick black outlines), referred to in the text as the northern, central and southern study regions.

At the SSI, information on the distribution and abundance of organisms and the structure of the ecosystem and environmental relationships is limited. Analyses of phytoplankton and zooplankton community structure and development (Liszka et al., this issue; Ward et al., 2004) and the distributions of fish and higher predator species along the island arc (Hart and Convey, 2018; Hollyman et al., this issue; Roberts et al., 2011) have suggested relationships with the large-scale ocean and sea ice environment of the SSI region. Furthermore, a recent macrobenthic assessment of the SSI also found the benthic biodiversity to be driven by environmental factors (Hogg et al., 2021).

Understanding marine ecosystems requires knowledge of both the local conditions and the wider regional connectivity of the ecosystem. Advection is a key component of Southern Ocean ecosystems that affects community structure, including that of the Scotia Sea (e.g., Hofmann and Murphy, 2004; Hunt et al., 2016; Murphy et al., 2016; Murphy et al., 2007). Observations and modelling studies have demonstrated connections across the Scotia Sea to the SSI, from areas including the southern ACC and northwestern Weddell Sea (e.g., Murphy et al., 2004; Renner et al., 2012; Robinson et al., 2017; Thompson and Youngs, 2013; Thorpe et al., 2007), but more detail is needed on the connectivity, both locally around the islands and within the wider Southern Ocean, to fully understand the operation of the ecosystem.

In this paper, we characterise the spatial and temporal variability of the marine environment of the SSI and its local and regional connectivity to improve understanding of the major drivers of the ecosystem structure and functioning in this region. We begin by describing the local water mass distribution along the SSI arc using data from the World Ocean Atlas 2018, a compilation of historical in situ data, and Argo float profile data. We then focus on key properties of the marine environment of the SSI, namely ocean temperature, seasonal ice cover, and surface chlorophyll concentrations, from the last decade which covers the operation of the Marine Protected Area and the period just prior to its establishment. Trajectories from near-surface satellite-tracked surface drifting buoys and Argo floats together with velocity fields and sea surface height data from a global reanalysis are used to extend current knowledge of the connectivity within the island arc and with the wider Southern Ocean.

2. Materials and methods

To investigate the marine environment of the SSI, we used a number of open access datasets. These provide data at high resolution for multiyear periods and permit characterisation of both the spatial and temporal variability in the region. All analyses and data visualisation were performed in Matlab R2020b, with use of the Climate Data Toolbox (Greene et al., 2019) and the M_map mapping package (Pawlowicz, 2020), using the cmocean (Thyng et al., 2016) and ColorBrewer (www.colorbrewer2.org) colour maps for visualisation.

2.1. Water mass properties and distribution

We used objectively analysed annual mean temperature and salinity data for the period 2005–2017 from the World Ocean Atlas 2018 (Boyer et al., 2018; Locarnini et al., 2019; Zweng et al., 2019) to describe the long-term mean water mass structure of the region. The World Ocean Atlas is a gridded dataset of quality controlled historical profile and surface data, including from ship-deployed, mooring, float and animal-mounted sensors, gridded at $1/4^\circ$ resolution on 102 depth levels from the surface to 5500 m. Temperature and salinity data from Argo float profiles (see Section 2.3) were used to depict seasonal and temporal variability.

2.2. Surface temperature, sea ice and chlorophyll *a*

To characterise spatial variability in the pelagic and upper ocean environment of the SSI arc, we examined sea surface temperature (SST),

sea ice concentration and surface chlorophyll *a* concentration from remotely sensed datasets for the period 2009 to 2020 or 2021, depending on dataset (see below). We defined three study regions of 1° latitude \times 2° longitude aligned along the SSI arc to describe the northern, central and southern areas of the arc, spanning $56\text{--}57^\circ\text{S}$, $28\text{--}26^\circ\text{W}$; $57.5\text{--}58.5^\circ\text{S}$, $27.5\text{--}25.5^\circ\text{W}$; and $59\text{--}60^\circ\text{S}$, $28\text{--}26^\circ\text{W}$ respectively (Fig. 1C). For each region, we calculated area-weighted monthly mean values of SST, sea ice concentration and chlorophyll *a*.

We used daily gap-filled fields of SST (at 20 cm depth) and sea ice concentration at 0.05° spatial resolution for the period 2009–2021 from the European Space Agency Sea Surface Temperature Climate Change Initiative (ESA CCI) and Copernicus Climate Change Service (C3S) reprocessed SST analyses v2.0 (Good et al., 2019, 2020; Merchant et al., 2019), made available by Copernicus Marine Service. Production of the ESA CCI and C3S SST fields uses sea ice concentration data from the Ocean and Sea Ice Satellite Application Facility (OSI-SAF; Lavergne et al., 2019) to mask areas of sea ice cover, and the sea ice data are provided with the SST data at the same temporal and spatial resolution.

We used monthly mean chlorophyll *a* fields at 4 km resolution from the reprocessed Copernicus GlobColour level 4 dataset, made available through the Copernicus Marine Service (Garnesson et al., 2019; Global Monitoring and Forecasting Center, 2021). In order to provide a product that is consistent over time, and thus suitable for time series studies such as ours, the GlobColour product merges ocean colour data from a suite of sensors. At high latitudes, ocean colour measurement is limited by low solar insolation in winter, and coverage can be restricted in other months due to cloud and sea ice cover. For the regional chlorophyll *a* time series, we retained only data points where at least 50% of the contributing grid cells had chlorophyll *a* data.

2.3. Float trajectories

To determine connectivity to the SSI, we used quality-controlled trajectories from near-surface satellite tracked drifting buoys (drifters) and Argo floats. The former are drogued at 15 m to track upper ocean current flows. All data are made available by the NOAA Global Drifter Program (Lumpkin and Centurioni, 2019). As part of quality control procedures, the drifter positions are optimally interpolated onto 6 hourly positions and the point of drogue detachment is determined (Lumpkin et al., 2017; Lumpkin and Pazos, 2007). We used trajectories of drifters that passed through $60.5\text{--}55.5^\circ\text{S}$, $29\text{--}25^\circ\text{W}$ ($N = 37$), discarding any data from drifters where their drogue was no longer attached. Drifter trajectories spanned the period 1995–2020.

Delayed mode Argo float trajectory and temperature and salinity profile data for floats that passed through the same area as for the drifter analyses were obtained from the Argo Global Data Center (Argo, 2000). Argo floats are autonomous, free-floating instruments that drift at a parking depth of ~ 1000 m and every 10 days profile the water column from depths of up to 2000 m to the surface, either as they ascend to or descend from the surface. Data are quality controlled by regional data centres and profile data are interpolated onto fixed pressure levels. We used only data that had quality control flags of 'good', excluding data from float trajectories which had interpolated locations, due, for example, to sea ice cover. An additional float that travelled from the southern Weddell Sea to close to the SSI was included to demonstrate transport connections between the two regions. In total, 30 Argo floats were used, covering the period 2003–2021.

2.4. Velocity fields and sea surface height

We used monthly mean velocity and sea surface height output from the Copernicus Marine Service global ocean eddy-resolving reanalysis, GLORYS12V1 (Global Monitoring and Forecasting Center, 2018). GLORYS12 provides an estimate of the state of the ocean by assimilating observations of sea level anomaly, sea surface temperature, sea ice concentration, and vertical profiles of in situ temperature and salinity

with a $1/12^\circ$ horizontal resolution version of the Nucleus for European Modelling of the Ocean (NEMO) platform that is forced at the surface with European Center for Medium-Range Weather Forecasts ERA-Interim and ERA5 reanalysis data. GLORYS12 has been shown to reproduce the velocity field of the ACC well in Drake Passage (Artana et al., 2021), and we therefore assume that it also reproduces the velocity fields well through the Scotia Sea extending to the SSI region.

We calculated climatological mean velocity fields from GLORYS12V1 output for the period 2010–2019. The GLORYS12V1 sea surface height data were used to examine potential variability in circulation, and hence connections, to and from the SSI. Sea surface height data have frequently been used to describe the circulation of the ACC and Weddell Gyre (e.g., Armitage et al., 2018; Kim and Orsi, 2014; Sokolov and Rintoul, 2009) and Reeve et al. (2019) have shown that the circulation of the Weddell Gyre derived from satellite data compares well with that constructed from Argo float data. Satellite-measured sea surface height is limited to sea ice-free regions, and although current research is focussed on estimating sea surface height from areas of sea ice cover (see Armitage et al., 2018 for an overview), the availability of such products is presently limited in time. Hence, we use sea surface height output from GLORYS12 to cover the period of interest in our study, with the caveat that sea surface height provided for ice-covered regions will be less robust than for the open ocean given the lack of data assimilation in these areas.

For each of the three study regions along the SSI arc (cf. Fig. 1C), we calculated the area-weighted mean sea surface height for each month for the period 2010–2019 (Fig. S1). We then extracted the monthly streamlines corresponding to the area-weighted values, by contouring the monthly mean sea surface height fields, to provide an indication of monthly mean flow pathways to and from the three study regions. All locations of the monthly streamlines were gridded to produce a frequency distribution field as a preliminary analysis of potential variability in the surface pathways to and from the SSI. To test the sensitivity of the results, we repeated the analysis using the minimum and maximum values of mean sea surface height for each study region rather than the mean value. We also repeated the analysis using mean sea surface height from summer only data (December–February) to confirm that there was no seasonal bias in the results from including the winter sea surface height fields.

3. Results

The results are described in two overarching sections: i) physical and biological oceanographic conditions including water mass properties (Fig. 2), sea ice (Fig. 3), and chlorophyll *a* fields (Fig. 4), and their seasonal and interannual variability (Fig. 5); and ii) local and regional oceanic connectivity to the SSI as determined from velocity fields (Fig. 6), drifter and Argo float trajectories (Fig. 7, Fig. 8), and the sea surface height analyses (Fig. 9).

3.1. Water mass structure and sea surface temperature

A meridional transect along 27°W extracted from the World Ocean Atlas 2018 illustrates the climatological mean water mass structure along the SSI arc and the distinction between the ACC and Weddell Gyre-influenced waters in the region (Fig. 2A). The SB, defined as the southern extent of Upper Circumpolar Deep Water, is located at $\sim 55.25^\circ\text{S}$ from the terminus of the subsurface 1°C isotherm (e.g., Venables et al., 2012) and coincides with the northward limit of winter sea ice extent (Fig. 3A). Cold Antarctic Surface Water (AASW) occupies the upper 100–150 m of the water column along the section, with Winter Water (WW), a remnant of AASW identified as a subsurface temperature minimum, beneath this. North of the SB, within the ACC, Circumpolar Deep Water (CDW) is found below the WW. At the northern end of the section, the warm core of Upper Circumpolar Deep Water, at approximately 400 m depth, has temperatures $>2^\circ\text{C}$ which decrease towards

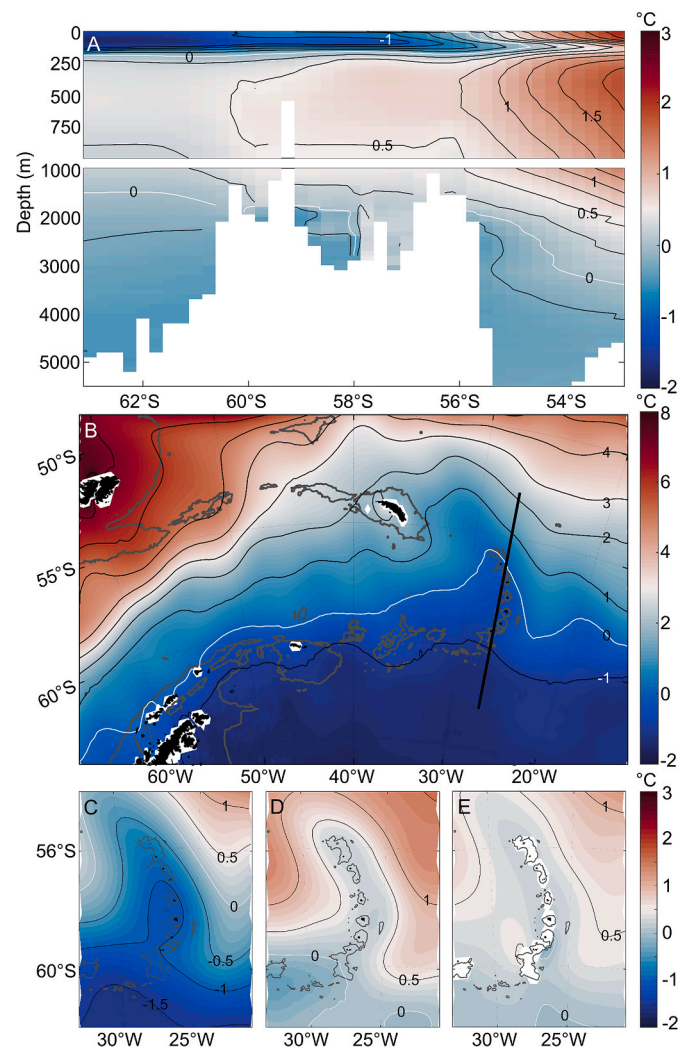


Fig. 2. Annual mean in situ temperature ($^\circ\text{C}$) for 2005–2017 from the World Ocean Atlas 2018. A) Vertical section of in situ temperature vs latitude for a north-south transect along 27°W , marked on B. White areas indicate bathymetry. Note the change in vertical scale at 1000 m. B) Surface temperature. C) Temperature at 100 m for the region around the South Sandwich Islands. D) As C but for 200 m. E) As C but for 1500 m. The 1500 m isobath is plotted in grey on B–E. In all panels, the 0°C isotherm is marked in white. Note the different temperature scale for panel B.

the SB. Beneath Upper CDW is Lower CDW, identified from its higher salinity core. South of the SB, Warm Deep Water (WDW) underlies the AASW and WW. CDW enters the Weddell Gyre at its eastern end and is modified during cyclonic transport in the gyre to become WDW (Orsi et al., 1993). Orsi et al. (1993) defined the northern limb of the WG as having WDW temperature maximum $>0.5^\circ\text{C}$, with colder water in the central gyre. Along the section at 27°W , this transition occurs at $\sim 60.5^\circ\text{S}$. The WDW north of this latitude has a reduced salinity ($S < 34.68$; not shown) compared with WDW to the south, an indicator of the WSC (Orsi et al., 1993). Hence, the SSI arc is an area of transition between the interior WG waters to the south of the island arc and the ACC to the north. Beneath the WDW and CDW, Weddell Sea Deep Water (WSDW) has temperatures $<0^\circ\text{C}$. WSDW occupies the lower 3000 m of the water column in the south of the section and decreases in volume northwards, entering the Scotia Sea through the Georgia Passage north of the SSI arc (Locarnini et al., 1993). The outflow of WSDW through sills and passages is constrained by its density and along the temperature section presented here, WSDW is only observed along the SSI arc in the deepest passages found north and south of Saunders Island that have

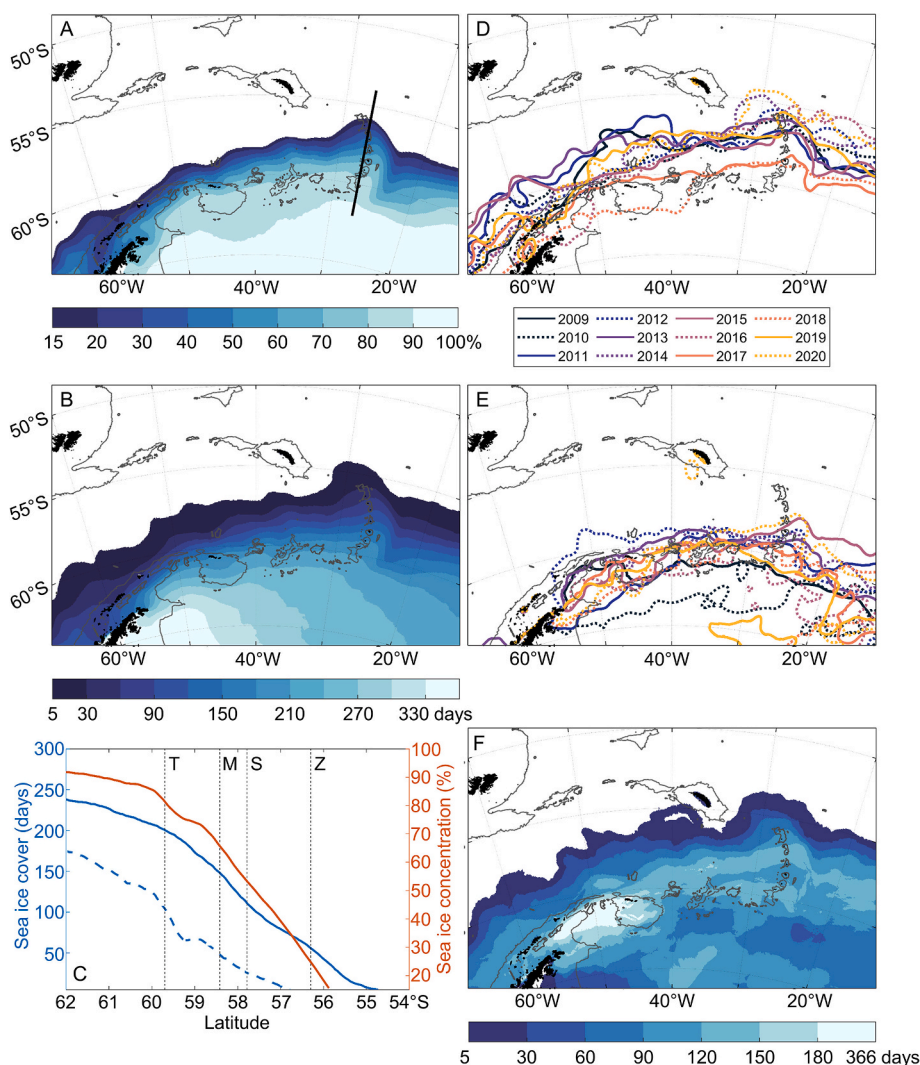


Fig. 3. Sea ice distribution in the Scotia Sea. A) Mean July–September sea ice concentration for 2009–2020. B) Mean number of days per year with sea ice concentration >15%, calculated from mid-February to mid-February for 2009/2010–2020/2021. C) Mean number of days of sea ice (solid blue line, sea ice concentration >15%), pack ice (dashed blue line, sea ice concentration >80%) and mean July–September sea ice concentration vs latitude (red line) for a north-south transect along 27°W, marked in A. The latitude of Southern Thule (T), Montagu (M), Saunders (S) and Zavadvoski (Z) islands are indicated with dashed lines. D) Sea ice edge (15% sea ice concentration) on 15 September 2009–2020. E) As D) but for 15 December 2009–2020. F) Range (difference between maximum and minimum) of number of days of sea ice cover per year for 2009/2010–2020/2021. The 1500 m isobath is marked in grey in the map panels. Sea ice data from ESA CCI and C3S (see text for details).

depths >2500 m, with coldest temperatures south of 58°S. The water mass structure along the island arc means that bottom temperature varies with depth. Onshelf, the less dense, warmer waters of WDW penetrate and temperatures are >0 °C. Offshelf, where the seafloor is deeper, temperatures are sub-zero.

The northeastward deflection of the ACC across the Scotia Sea and its return south to the east of the SSI, and the northward extension of the Weddell Gyre-influenced waters across the SSI arc, are apparent in the horizontal temperature fields (Fig. 2B–D). At the surface, annual mean temperatures range from approximately 0 °C at Protector Shoal at the northern end of the SSI to < -1 °C in the northern limb of the Weddell Gyre (Fig. 2B). At 100 m, in the WW layer, temperatures are < -0.5 °C at the north of the island arc, decreasing to < -1 °C from Saunders Island to the south (Fig. 2C). Below the AASW and WW layer, temperatures increase in the CDW and WDW, with a smaller range in temperature along the SSI than at shallower depths. Above and below the temperature maximum layer of the CDW and WDW, temperatures are similar at 200 m and 1500 m (Fig. 2D and E). There is a large zonal temperature gradient across the island arc caused by the deflection of the ACC, with warmer waters to the west and east of the islands. The gradients appear strongest in the 100 m and 200 m fields, with a sharp eastward incursion of warmer water towards Saunders Island evident at 200 m. Because of the water mass distribution, horizontal temperature gradients are greater longitudinally across the island arc than latitudinally along the arc.

Smaller scale and seasonal variability in water mass properties in the SSI region is evident from Argo profile data (Fig. S2). The Argo floats provide good coverage of the northern part of the SSI in particular, with profiles taken in all seasons. Surface temperatures range from freezing point to >2.5 °C and surface salinity from 33.4 to >34.6 (Figs. S2A–C), with surface properties modified seasonally and interannually by sea ice distribution and air-sea fluxes. The depth of the subsurface temperature minimum, which corresponds to WW, indicates the depth of mixing in the previous winter (Fig. S2D), and ranges from ~50 m around the islands to 200 m in the ACC waters northeast of the SSI. The properties of the WW change across the region, with colder and fresher WW found near the central SSI (Saunders Island to Visokoi Island) (Figs. S2A–C). Below the WW, the differences in the temperature of the temperature maximum illustrate the influence of ACC and Weddell Gyre waters. WDW is coldest in the shelf areas along the island chain. Although still cold, the temperature maximum southeast of the islands is warmer than along the island chain, suggesting waters from the central Weddell Gyre region. Warmer temperatures (>1 °C) associated with Upper CDW are observed to the west of the island arc and in the northeastern profiles where temperature approaches 2 °C, indicative of the presence of the Southern ACC Front. At 1500 m (Fig. S2B), the zonal gradient in temperature noted in the climatology is clear with coldest temperatures around the island chain and temperature increasing away from the islands to the west and east, with warmest temperatures in the northeast of the region and coldest waters in the southeast.

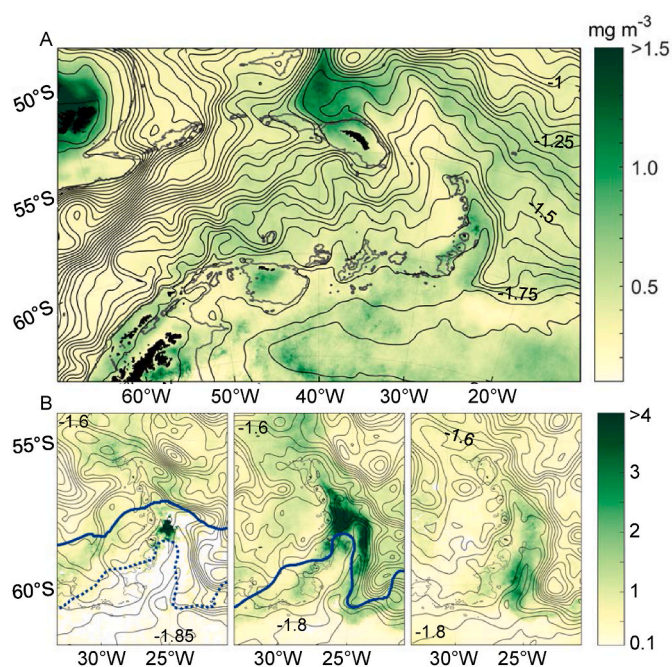


Fig. 4. Surface chlorophyll *a* concentration (chl *a*; mg m⁻³) overlaid with isolines of sea surface height (m). The sea surface height isolines indicate circulation streamlines; flow is parallel to the contours with lowest values of sea surface height to the right of the flow in the Southern Hemisphere and steep gradients in the contours indicating stronger flow. A) Climatological summer mean chl *a* (December–February) for 2009–2020. B) Monthly mean chl *a* for December 2015 (left), January 2016 (middle) and February 2016 (right). Also marked on B is the sea ice edge (15% concentration) on the first and last day of the month (solid and dashed blue lines respectively). Sea ice has retreated from the region before the end of January 2016. Note the different colour scales for A and B. Chl *a* data from GlobColour, sea surface height data from GLORYS12V1, sea ice data from ESA CCI and C3S (see text for details).

The seasonal cycle in sea surface temperature (SST) along the SSI arc is well defined, with maximum temperatures in February and minimum temperatures in August to September (Fig. 5A). In summer, median temperatures decrease southwards from 1 °C in the northern region to 0.5 °C in the south, with an interannual range of ~1 °C across all regions. In winter, the median SST is < -1.5 °C in all regions, with less variability than observed in summer. Removing the seasonal cycle in the SST time series allows us to understand the relationship in interannual variability across the SSI arc. The de-seasonalised SST fluctuations are strongly positively correlated between the three regions ($R > 0.78$, $p < 0.001$). Years when summer temperatures were warmer than normal in all regions (2009/10, 2010/11, 2016/17 and 2019/20) coincide with the sea ice being south of the island arc in those summers (Fig. 3E, Fig. 5B). There is also additional spatial variability in the difference in temperatures across the regions within years, with a smaller difference in temperature between the three regions in some years (e.g. summers of 2009/10, 2013/14 and 2020/21) than in other years (e.g. summers of 2011/12 and 2015/16). This suggests that local processes, in addition to the larger scale circulation, strongly influence SST across the SSI.

3.2. Sea ice

The seasonal sea ice cycle exerts a strong seasonality on the SSI, with winter sea ice extending on average across the SSI arc (Fig. 3). Mean July–September sea ice concentration decreases northwards from pack ice (sea ice concentration >80%; Stroeve et al., 2016) in the northern Weddell Sea to mean concentration <20% at the northern end of the SSI arc (Fig. 3A). The timing of advance and retreat of the sea ice across the island chain causes a large north-south difference in annual sea ice cover

along the island arc, with an average of 30–60 days of sea ice cover in the north compared with >180 days in the south (Fig. 3B). As a result, each of the islands of the SSI arc experiences a different pattern of seasonal sea ice dynamics (Fig. 3c, Fig. 5B). In the south, the sea ice season is long, typically from June to December, with earlier northward advance and later retreat in this region than further north along the island arc. From June to November, average sea ice concentration exceeds 50% with pack ice present from July to October (Fig. 5B). The Southern Thule group has ~7 months of sea ice cover with on average ~3 months of dense pack ice cover, with an average winter concentration of ~80% (Fig. 3C). In the central SSI region, which includes Saunders and Montagu islands, the sea ice season is shorter than further south, generally lasting from July to November, with peak sea ice cover occurring in August and median winter sea ice concentration of ~70%, with ~1 month where median sea ice concentration exceeds 80%. In the northern region of the SSI, around Zavadovski and Visokoi islands, sea ice is typically present only for ~2 months in August–September, with median winter sea ice concentration <40%.

Associated with the mean seasonal cycle in sea ice is large interannual variability, with considerable differences in the timing of the sea ice advance and retreat, and its distribution between years (Fig. 3D and E, Fig. 5B). This variability results in a difference in maximum and minimum annual days of sea ice cover of 60 to >120 days across much of the island arc (Fig. 3F). The northern and central islands of the SSI are towards the northward limit of sea ice extent, and as a result there is a large range in winter sea ice extent and concentration (see also Fig. 5B, Fig. S3). For example, September sea ice extent was further north than usual in 2014 and 2020, resulting in years of above average sea ice concentration around the northern SSI (Fig. 3D and E, Fig. 5B). In 2017 and 2018, the sea ice only extended to Montagu Island in mid-September, so the northern and central islands had less sea ice cover than usual. In the southern region of the SSI, the lowest winter sea ice concentration occurred in September 2017 following the early retreat of the sea ice that year. There is large variability in the timing and rate of sea ice advance, particularly during May and June, which results in autumn/early winter sea ice concentration ranging from no sea ice (2011, 2013, 2018, 2019, 2020) to >80% concentration (2014, 2016) in the southern region of the SSI. Likewise, the relationship between late winter and early summer sea ice extent is not straightforward, with complexity in the rate and direction of sea ice retreat. In December, the northern islands are ice-free in all years considered here, but there is considerable variability around the central and southern islands with the summer ice edge varying from north of Saunders Island in some years (2015 and 2020) to south of the island arc in 2010 which impacts the duration of the sea ice season in these regions.

As expected, the seasonal sea ice cycle is inverse to that of SST with maximum sea ice cover in the three regions in July to September and minimum cover in the austral summer (Fig. 5A and B). While SST and sea ice concentration are linked on short time-scales, there does not appear to be a straightforward relationship between SST and sea ice concentration in consecutive years. In some years, reduced sea ice concentration follows a warm summer. For example, there was less sea ice in the northern region in the winters of 2011, 2017 and 2018 after higher than usual summer temperatures. Yet, in winter 2020, sea ice concentration in both the northern and central regions was relatively high despite the summer of 2019/20 being anomalously warm. Likewise, more extensive sea ice cover in winter does not necessarily lead to cooler surface temperature the following summer.

3.3. Chlorophyll *a* concentration

Mean summer chlorophyll *a* concentration illustrates the generally high productivity of the Scotia Sea (Fig. 4A) with intense blooms around South Georgia and increased productivity within the area of winter sea ice cover (cf. Fig. 3) in the southern ACC and the Weddell Sea in agreement with earlier studies. Elevated levels of chlorophyll *a* occur at

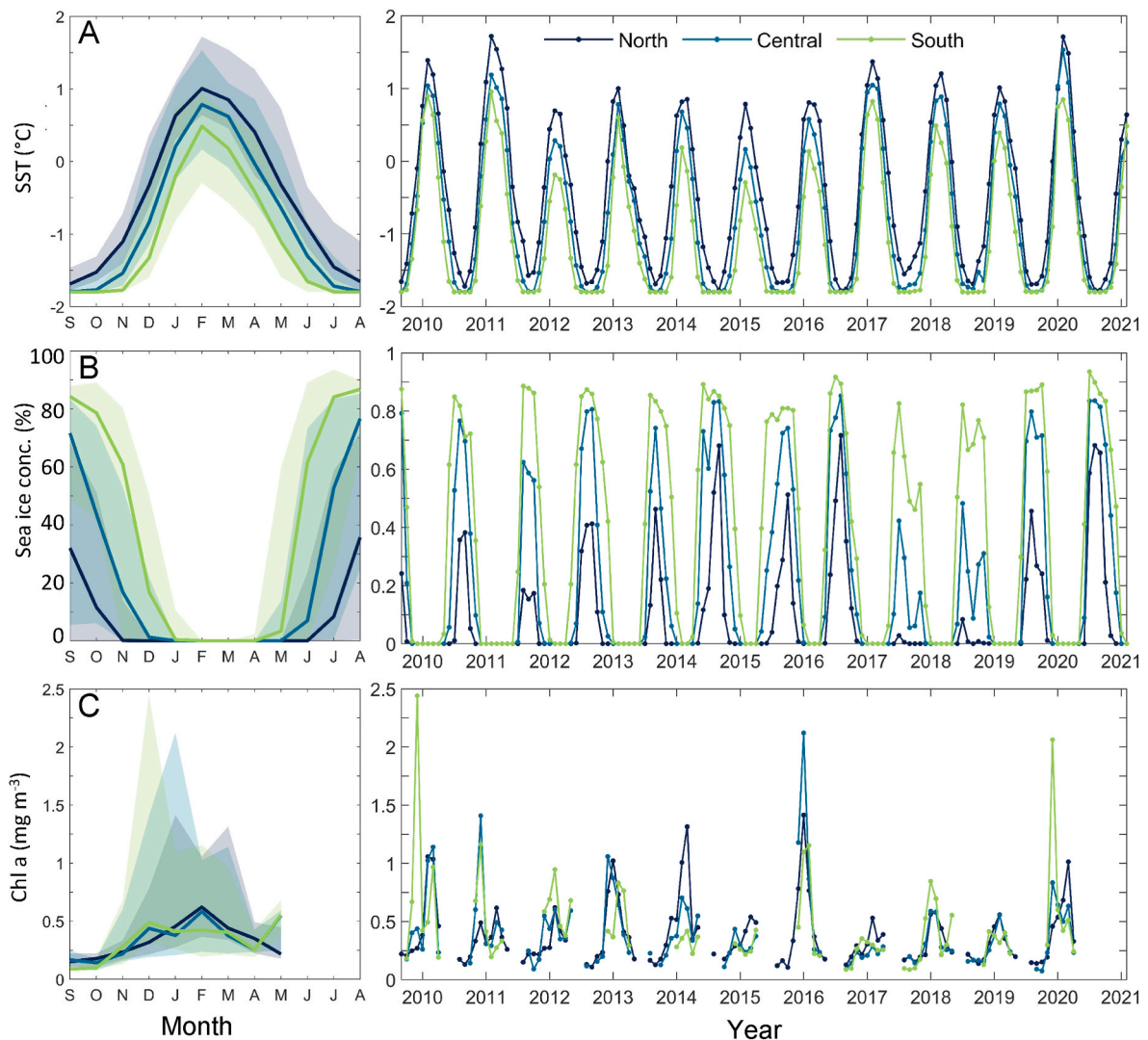


Fig. 5. Seasonal cycle and interannual variability in monthly mean properties for the northern, central and southern regions of the South Sandwich Islands (marked on Fig. 1C). A) Sea surface temperature (SST; °C). B) Sea ice concentration (%). C) Surface chlorophyll *a* concentration (chl *a*; mg m⁻³). Only data for months with >50% chl *a* data coverage are plotted which means the winter season is not resolved. Left-hand panels show median seasonal cycle (thick lines) and range (shaded). Values have been area-weighted according to underlying grid cell size in each region. SST and sea ice data from ESA CCI and C3S, and chl *a* data from GlobColour (see text for details).

the tip of the Antarctic Peninsula, on the South Orkney Plateau and in the northern Weddell Sea, and a band of relatively high chlorophyll *a* (>1 mg m⁻³) extends along the SSI arc, continuing to the east and then south. Comparison of the chlorophyll *a* field with the current streamlines illustrates the connection between the spatial extent of the chlorophyll blooms and the regional currents, as previously described for the South Georgia bloom (e.g., [Borrione and Schlitzer, 2013](#); [Venables et al., 2012](#)). The southward deflection of the ACC east of the SSI appears to bound the distribution of increased chlorophyll around the island chain, with lower chlorophyll to the east of the strong flow.

While the mean summer data show generally increased chlorophyll *a* around the SSI, the available monthly mean chlorophyll *a* data illustrate the spatial and temporal variability in surface productivity in the SSI region (Fig. 5C, Fig. S3). Peak chlorophyll *a* concentrations typically occur in December to March, but location, spatial extent and magnitude of the blooms vary and timing is not consistent between regions or from

year to year. Maximum area-weighted monthly mean values > 2 mg m⁻³ were observed in December 2009 and December 2019 in the southern region, and in January 2016 in the central region, while chlorophyll *a* concentrations remained relatively low in all regions in 2014/15, 2016/17 and 2018/19.

Monthly mean chlorophyll *a* fields for 2010–2020 show that primary productivity can respond rapidly to the retreat of the sea ice with blooms frequently occurring within the same month that sea ice retreats, with variability in the sea ice field contributing to the variability observed in the surface chlorophyll (Fig. S3). In summer 2015/16, for example, an intense localised bloom in the central Scotia Sea region followed later-than-usual sea ice retreat (Fig. 4B). Sea ice remained anomalously far north in November 2015 and, at the start of December, the sea ice edge was north of Saunders Island. During December, the sea ice retreated to the southern end of the island arc, and a bloom formed east of Saunders and Montagu islands. Comparison of the chlorophyll *a* concentration

field in January 2016 with surface current streamlines suggests that the bloom was advected northwards by the current flows along the SSI and then southwards in the return flow east of the island arc. Elevated chlorophyll *a* concentrations remained in February 2016 with the main area of the bloom located southeast of the SSI. A close relationship between bloom propagation and the surface circulation can be seen in the development of the surface blooms through the time series (Fig. S3).

3.4. Connectivity

3.4.1. Local circulation and connectivity

High resolution current fields from the GLORYS12 reanalysis illustrate the spatial complexity of the circulation around the SSI (Fig. 6, cf. Fig. 1C). At 200 m, strong flows approach the islands from the west and split into several branches, steered by the bathymetry and channelled through passages between the islands (Fig. 6A). A northern branch that enters the region at $\sim 57^\circ\text{S}$ follows a southward loop towards Saunders Island before retroflecting northwards along the western side of the island arc. Further south, currents diverge at $\sim 58^\circ\text{S}$ to the west of the channel between Saunders and Montagu islands and separate into northward and southward branches. A strong northeastward current between Zavadvovski and Visokoi islands results from the northward flow being steered eastwards by Leskov Island. Eastward flows are also evident through the passage south of Montagu Island, and through those north and south of Saunders Island where the seamounts west of Saunders Island appear to be important for bathymetric steering. These latter passages are the deepest passages between the islands with depths >2000 m (cf Fig. 1C). East of the island chain, there is again divergence in the flow fields, with northwards flow along the eastern continental shelves of Saunders Island and the islands north, and southward flow from Montagu Island and around Tyrell Bank at the southern end of island arc before northward deflection. Further offshore to the east, the circulation links to the southward current jet associated with the SB.

The currents at 1000 m are generally slower than at 200 m, although

the northward flow along the eastern side of Saunders Island has strengthened with depth so that the currents are faster than at 200 m (Fig. 6B). This stronger band of northward currents is deflected away from the northern islands at 57°S , suggesting there may be little connection between the southern and northern islands at this depth. The eastward flow between Zavadvovski and Visokoi islands, although still present at 1000 m, has weakened relative to 200 m and the currents along the eastern shelf of Montagu Island and the southern islands are slower than observed at 200 m. Offshore of the southern islands, the flow is concentrated into a relatively broad zone of northward flow along the western edge of the South Sandwich Trench. This current retroflects at $\sim 57.5^\circ\text{S}$ to continue southwards along the eastern side of the trench, as indicated in the surface current streamlines (Fig. 4). The current fields indicate some westward flow from this jet towards Saunders Island at $\sim 58^\circ\text{S}$ around the northern side of Montagu Bank to the east of Montagu Island, which is then deflected north by the bathymetry. Currents along the eastern side of the northern islands are steered eastwards and join the southward flow along the trench.

The passages north and south of Saunders Island are the only locations where water at 2000 m can cross the SSI arc, and there is only weak flow through these in the climatological velocity field at 2000 m (Fig. 6C). The northward flow along the western edge of the South Sandwich Trench remains strong at this depth with the westward connection towards Saunders Island and then northwards onto Visokoi and Candlemas islands still apparent. The currents are deflected away from Zavadvovski Island by the bathymetry to the east of the island and join the southward flow along the trench. One other feature of note is an area of cyclonic recirculation at the northern end of the trench which increases in strength with depth. This is located close to the deepest point of the trench.

Local pathways of transport within the SSI arc are further illustrated by the near-surface drifter and float trajectories (Fig. 7). Near-surface drifters show northward transport from the southern islands, traveling from Southern Thule via Montagu and Saunders islands before

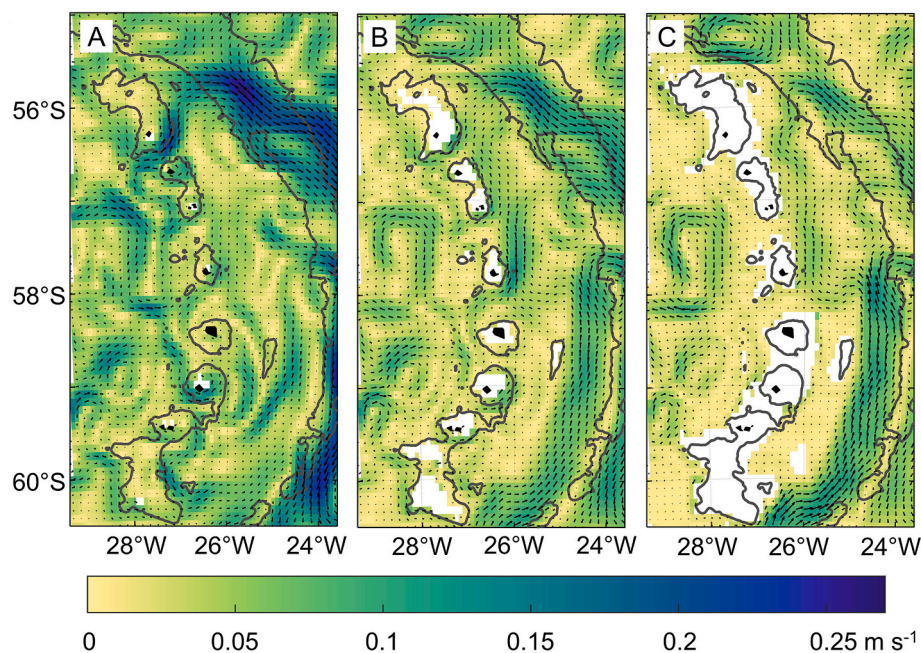


Fig. 6. Annual mean currents (m s^{-1}) for 2010–2019 around the South Sandwich Islands at A) 200 m, B) 1000 m and C) 2000 m. Current speed is shaded and vectors show direction. 1500 m and 6000 m isobaths are marked on all panels (grey lines). Current data from GLORYS12V1 reanalysis (see text for details).

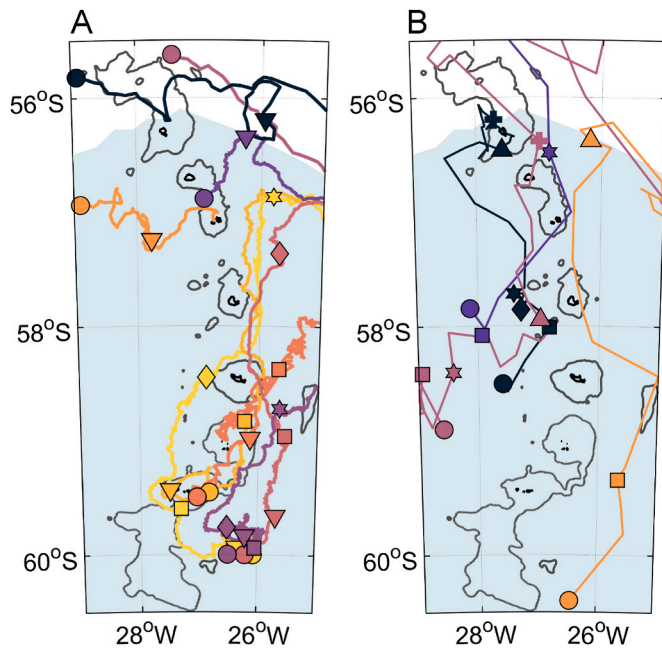


Fig. 7. Trajectories of selected A) near-surface drifters (15 m depth) and B) Argo floats (~1000 m depth) around the South Sandwich Islands. Deployment locations are marked with a circle and time intervals from deployment are indicated by symbols: 10 days (downwards triangle), 30 days (square), 60 days (diamond), 90 days (star), 180 days (upwards triangle) and 270 days (plus), coloured according to individual trajectories. Note that 10 day markers are only plotted in A. The 1500 m isobath is marked (grey lines) and the median winter sea ice extent for 1981–2010 is shaded as per Fig. 1A.

being deflected to the east, away from Vindication and Candlemas islands, at 57°S. Transport from Southern Thule to Montagu Island takes 20–30 days, and 10 days from Montagu Island to Saunders Island. At the northern islands, transport to the east is rapid, with transport from west of Zavodovski Island to east of the island arc taking 10 days. Areas of retention are also illustrated by the drifter trajectories. In the southern region, east of Tyrell Bank, a drifter was retained by an eddy for approximately 30 days before travelling north along the island arc. High frequency variability in the circulation between Bristol and Montagu islands also increases retention with a drifter retained in the local area for approximately 20 days.

The Argo float pathways correspond to the dominant features observed in the velocity fields and illustrate the slower transport times at depth as compared with the near-surface circulation (Fig. 7B). One float was advected northwards from Tyrell Bank to Saunders Island, following the flow along the western side of the trench and its westward deflection, before joining the southward flow of the SB east of Zavodovski Island after approximately six months. Floats on the western side of the island arc were transported northwards, with one float travelling through the passage north of Saunders Island and continuing along the eastern shelf of Visokoi and the Candlemas islands group, and another following the western side of the arc to reach Visokoi Island. For both floats, the corresponding travel time was 2–3 months. Areas of retention

are also related to the local bathymetry. One float was retained around the seamounts west of Saunders Island for approximately two months and again around Zavodovski Island for another three months.

3.4.2. Regional connectivity to the South Sandwich Islands

Near-surface connectivity to the SSI from the southern ACC through Drake Passage and from the northern Weddell Sea is illustrated with drifter trajectories (Fig. 8A). Transport pathways exist from the Antarctic Peninsula, South Orkney Islands, eastern South Scotia Ridge and South Georgia to the SSI on timescales of 1 to >9 months. Several of the drifters that reach the SSI have come from areas that could be under sea ice during winter.

There is broad regional connectivity to the SSI at depth (Fig. 8B). Some of the Argo float trajectories correspond to those of the near-surface drifters, with transport connections from the tip of the Antarctic Peninsula, the eastern South Scotia Ridge and South Georgia, but there is also transport from further north in Drake Passage and Burdwood Bank, from north of South Georgia and from the southern Weddell Sea. The floats that travel around the South Georgia shelf, or come from the north of South Georgia, are advected past the northern end of the SSI arc and southward in the flow along the eastern island arc. Floats take approximately 18–24 months from the central and southern Scotia Sea and 12 months from the northwest Weddell Sea to reach the SSI, with transport from 0°E in the southern Weddell Sea taking >5 years (Fig. 8E). Local features in the circulation can modify the transport times. The float deployed on the eastern South Scotia Ridge, for instance, was retained for almost four years in recirculation associated with a Taylor column, a columnar feature generated from interaction of flow with a bathymetric obstacle (Meredith et al., 2015). As with the drifters, the Argo floats also demonstrate potential connections from areas of winter sea ice cover to the SSI.

3.4.3. Regional connectivity from the South Sandwich Islands

Downstream of the SSI, the near-surface drifter trajectories initially demonstrate two main branches of onward transport (Fig. 8C): a northern branch that takes drifters directly east, and a second branch associated with the southward flow of the SB east of the SSI arc. Drifters caught in this latter current flow were then advected east in the flow along the South Sandwich Fracture Zone. Downstream of 0°E, the trajectories of two drifters that initially followed the southern branch of flow diverged, with one drifter remaining south and the other taken past the Crozet Islands, indicating that there is the possibility of transport from the seasonal sea ice zone to that region.

The two main transport pathways exiting the SSI region are also evident in the Argo float trajectories (Fig. 8D). Both datasets demonstrate connection from the SSI to islands downstream and back into areas of winter sea ice cover. Near-surface drifters that passed close to the SSI reached Bouvet and Crozet Islands in timescales of <6 months and >12–18 months respectively. Argo floats from the SSI passed Bouvet, Marion and Prince Edward Islands, and Kerguelen Islands after approximately 1, 2 and >6 years respectively, connecting areas of deeper bathymetry en route. The float trajectories are also consistent with the southward return loop at the eastern end of the Weddell Gyre (e.g. Orsi et al., 1993), with a float taken directly south at 25°E, and illustrate additional areas of retention in the local circulation. At ~52°S, 40°E, a float was caught for approximately a year near Ob' Seamount and Conrad Rise, contributing to a transport time to 50°E of approximately 5 years.

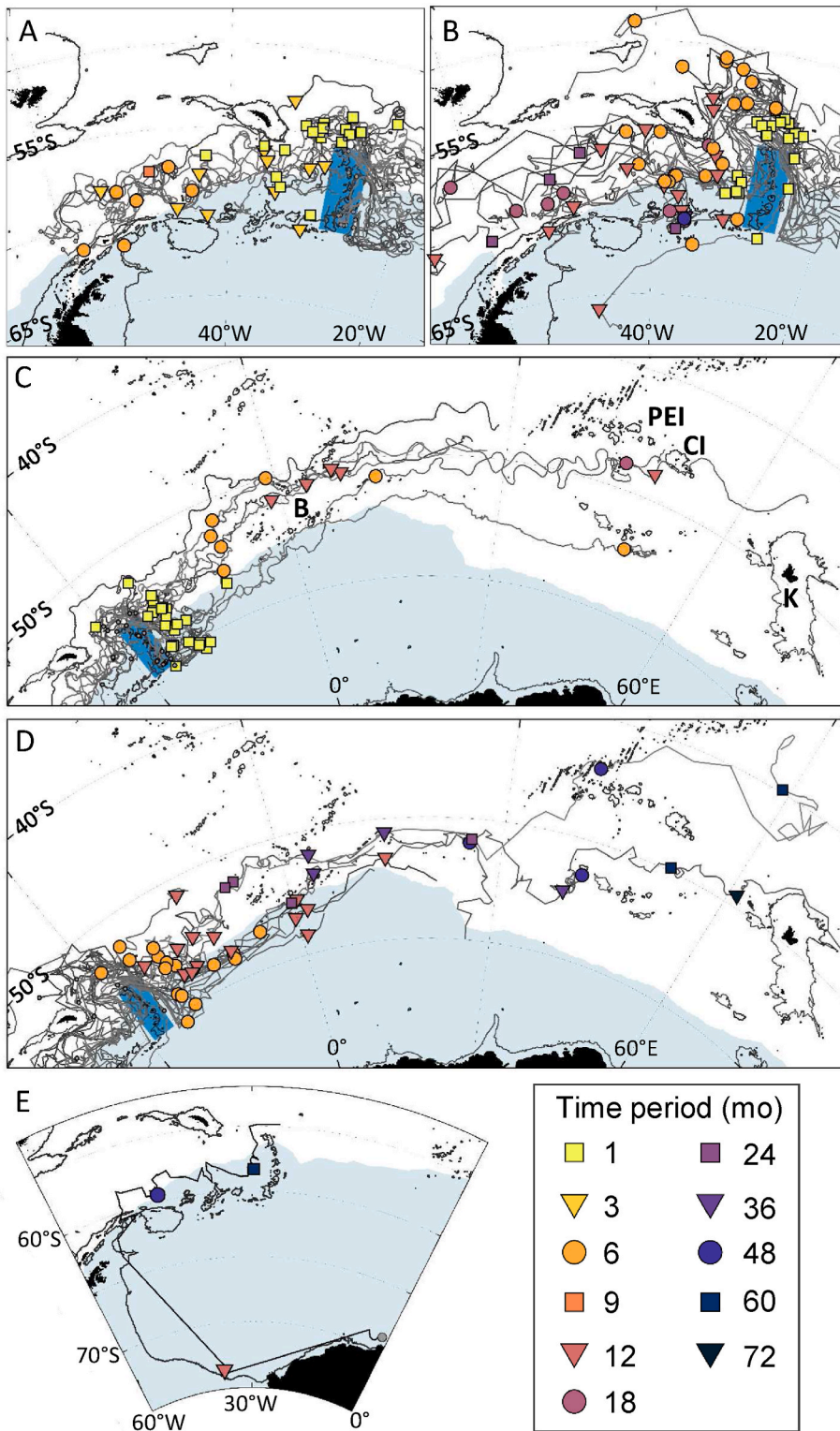


Fig. 8. Trajectories of near-surface drifters and Argo floats around the South Sandwich Islands (SSI). A) Near-surface drifters (15 m depth; grey lines) that travel through the SSI region (shaded in dark blue). Grey circles indicate deployment locations and coloured symbols mark the travel time (months) to the SSI region, according to the legend. B) As A but for Argo floats (~1000 m depth). C) Near-surface drifters that exit the SSI region. Coloured symbols indicate transport time (months) from leaving the SSI region, as per the legend. D) As C but for Argo floats. E) Argo float 7900078 that travelled from the southern Weddell Sea to the SSI. Note that not all time markers are shown in each panel. Median winter sea ice extent for 1981–2010 is shaded as per earlier figures and the 1500 m isobath is plotted in grey. Islands marked on C are Bouvet Island (B), Prince Edward and Marion Islands (PEI), Crozet Islands (CI) and Kerguelen Islands (K).

3.4.4. Variability in connectivity

Using streamlines generated from the mean value of sea surface height from the three study regions along the SSI (Fig. 1C) permits a visualisation of the broad distribution of surface transport pathways to the SSI arc (Fig. 9). The sensitivity test using streamlines derived from the minimum and maximum sea surface height values from each study region provides support for the overall conclusions from using the mean

values, while demonstrating the range in potential connections to each region (Fig. S4). Connections from South Georgia, for example, are indicated to be to the northern part of the SSI arc, in agreement with the drifter and float trajectories.

Streamlines to the northern region of the SSI tend to be from the western side of the Antarctic Peninsula and north of the South Orkney Plateau, with increased variability in the eastern Scotia Sea (Fig. 9A, D).

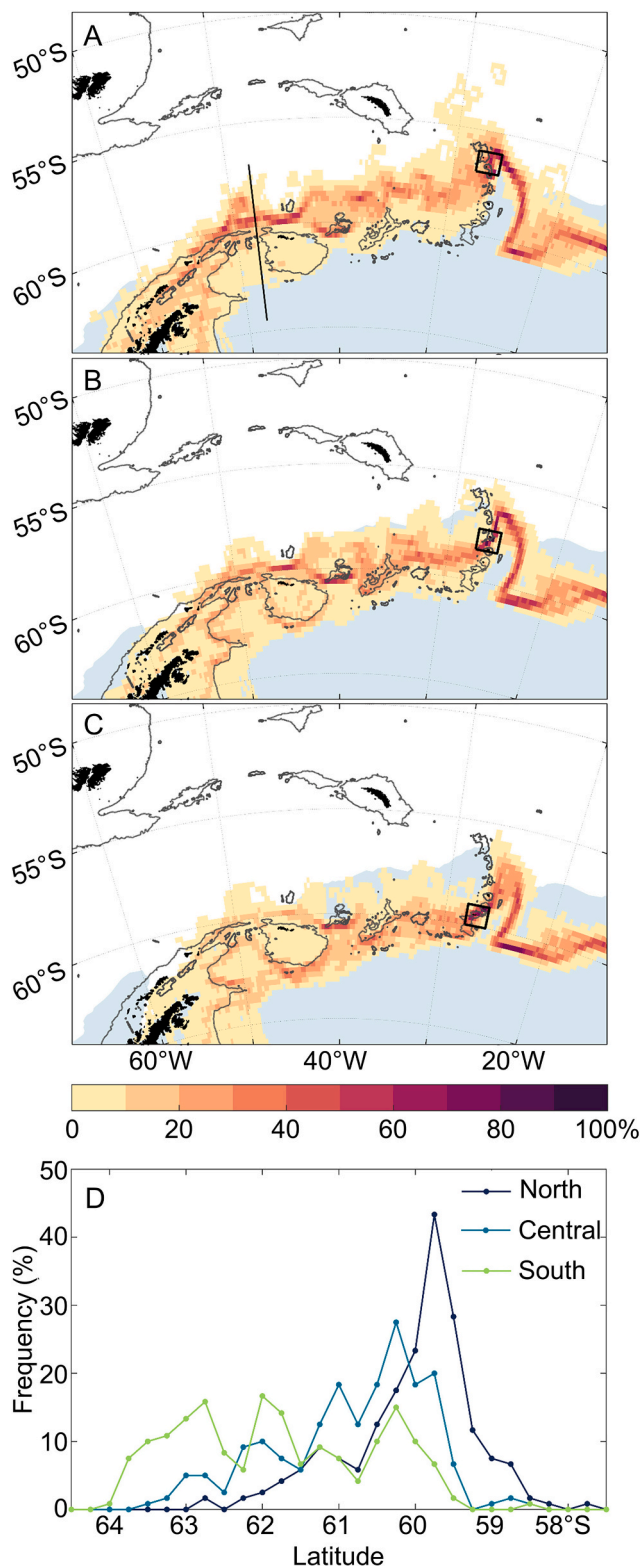


Fig. 9. Sea surface height variability as a proxy for connectivity to the South Sandwich Islands (SSI) calculated from monthly mean sea surface height data for 2010–2019. A) Northern SSI region. B) Central region. C) Southern region. Shading indicates frequency of pathways to each of the study regions (boxes marked on each panel, also see Fig. 1C), gridded at 0.25° horizontal resolution. The median winter sea ice extent for 1981–2010 is shaded as per earlier figures and the 1500 m isobath is plotted in grey. D) Latitudinal transect of frequency of pathways to each of the study regions along 48°W (black line in A). Sea surface height data from GLORYS12V1 (see text for details).

Pathways to the central SSI tend to be from southern areas towards the South Scotia Ridge, with potentially less input from the Western Antarctic Peninsula. One of the key transport routes to the central region is still to the north of the South Orkney Plateau, but there is more frequent input from the South Orkney Plateau and along its southern edge (Fig. 9B, D). There is a stronger connection from the Weddell Sea to the southern SSI region (Fig. 9C and D), although some connection from the Bransfield Strait along the northern Antarctic Peninsula and the southern ACC remains. Transport pathways appear to be more closely centred on the South Scotia Ridge east of the South Orkney Islands for this region.

The flow pathways from the three study regions defined along the SSI also vary on the eastern side of the SSI arc. From the northern region (Fig. 9A), the dominant transport route is southwards in the currents associated with the SB, whereas transport from the central and southern regions is initially northwards along the eastern side of the island arc before turning southwards (Fig. 9B and C). These results agree with the drifter trajectories (Figs. 7 and 8). At the southern end of the South Sandwich Trench, the circulation is strongly constrained along the west-east aligned South Sandwich Fracture Zone.

Extending the analyses to include the Weddell Gyre (Fig. S5) shows that the streamline analysis does not fully capture the transport pathways illustrated by the near-surface drifters, which are subject to additional surface forcing and smaller-scale processes than will be resolved in the GLORYS12v1 reanalysis product. Nevertheless, the results suggest that return flow in the Weddell Gyre is possible from all three of the SSI study regions. Connectivity from the SSI to the seamount of Maud Rise (~65°S, 3°E) occurs from all regions, but the probability of transport from Maud Rise appears to be greater for the southern region of the SSI. There are additional areas of sensitivity within the connectivity bounds, with increased possibility of eastward connection to East Antarctica from the northern region than from further south.

4. Discussion

We have examined the spatial and temporal variability and connectivity of the marine environment of the SSI. This quantified characterisation provides a framework for understanding how the environment influences the structure and functioning of ecosystems along the island arc. In the following sections we consider the spatial and temporal variability of the environment and the role of connectivity. We conclude by considering the ecological implications, including the potential impacts of change, and priorities for future research.

4.1. Spatial and temporal variability

The marine environment of the SSI arc is spatially complex. The SSI arc is one of the main barriers to the circumpolar flow of the ACC away from the Antarctic continent and the bathymetry of the island arc dominates the large-scale ocean circulation by deflecting the ACC to the north. This results in the SB occurring at its maximum northward extent in the Southern Ocean; there are only two locations where the SB is north of ~55°S: at the SSI and south of the Agulhas Basin (Orsi et al., 1993; Park and Durand, 2019). The northward deflection of the SB by the SSI permits northward penetration of Weddell Gyre waters into the SSI region, creating a strong thermal gradient between the island arc and the ACC waters present to the west and east. This occurs over a very narrow longitudinal range of ~5–10°, equivalent to ~300–600 km. ACC waters are brought close to the western side of the island arc, particularly at intermediate depths where the ACC appears to extend further east. There is also a smaller north-south temperature gradient along the SSI with temperature decreasing to the south with closer proximity to more central Weddell Gyre waters (Orsi et al., 1993). At depth, the complicated bathymetry of the island arc controls the pathways of the deep waters. We found indications that WSDW can enter the deep passages in the SSI arc, notably that south of Saunders Island, as proposed

by Naveira Garabato et al. (2002), but note that additional in situ observations are required to corroborate this. The local distribution and transport routes of WSDW around the SSI are uncertain but it would be useful to define these in more detail to better understand its potential influence on the ecosystem structure of the SSI, including, for example, how resultant temperature gradients affect the deep water community structure (e.g. Clarke et al., 2009; Hollyman et al., this issue; Roberts et al., 2011).

The mean locations of the circumpolar ACC fronts have recently been updated based on altimetry data (Park and Durand, 2019, Fig. 1), and depict the SB extending north of 54°S at the longitude of the SSI arc. This is in contrast to our results based on World Ocean Atlas and Argo float profile data. We found the SB to lie south of 55°S, closer to the northern end of the SSI arc (cf. Brandon et al., 2004; Liszka et al., this issue; Venables et al., 2012) and to approach more closely the western side of the island arc, indicating that the SSI will be influenced by water masses of the southern ACC as well as the Weddell Gyre. To the east of the SSI, climatological mean locations of the SB suggest the possibility of two eastward branches in the SB, one at ~57.5°S (Park and Durand, 2019, Fig. 1) and one further south at ~61°S (Orsi et al., 1995), coincident with the South Sandwich Fracture Zone. The velocity fields and drifter and float trajectories suggest both major pathways exist with flow converging downstream of 0°E.

Local interactions between the ocean circulation and bathymetry of the island arc introduce additional complexity to the environment. The bathymetry of the island arc is complex, with steep submarine slopes to the islands, narrow continental shelves <10 km wide that are typically <200 m deep although not all have been well surveyed, passages of varying depth and width between the closely spaced islands, and a number of seamounts and submarine banks (Leat et al., 2016). These interactions generate mesoscale and sub-mesoscale features in the ocean circulation and areas of intense mixing (Jiang et al., 2019), as well as local retention through bathymetrically driven features including Taylor columns (Meredith et al., 2015). The sharp retroflection in ACC flow on the periphery of the island arc will also impact local dynamics, producing additional mixing. There are also local physical processes that will add to the local dynamics including heat and nutrient flux from ongoing volcanic activity and glacial freshwater input, particularly from the more heavily glaciated islands in the south (Leat et al., 2014); the impact of these require further investigation.

Our analyses have demonstrated that temporal and spatial variability is a fundamental feature of the SSI marine environment. On top of the seasonal cycle in SST and the general north-south gradient along the island arc, there is interannual variability in surface temperatures, particularly in summer. A strong north-south gradient in the duration and density of sea ice also exists along the islands, with little sea ice and short sea-ice duration in the north, and heavy sea ice and a longer sea ice duration in the south. However, sea ice distribution, concentration and the timing and rate of advance and retreat were not consistent during our ~10 year study period, and there was substantial variability in the number of ice-free days experienced along the island arc. While at seasonal and shorter timescales the variability in SST and sea ice conditions within regions of the island arc are directly linked, the relationships between the regions within seasons and over longer timescales do not appear to be simple. The physical environment of this region is affected by local and large scale atmospheric drivers of variability, including the Southern Annular Mode (SAM) and El Niño Southern Oscillation (ENSO), which affect the upper ocean and the advance, retreat and drift of sea ice and lead to large scale temperature and sea ice anomalies across the region (e.g., Meredith et al., 2005; Murphy et al., 2014; Murphy et al., 2007; Stammerjohn et al., 2008). Understanding the impact of these drivers on the variability in this region is a key next step for future research.

We found the location and timing of surface phytoplankton bloom formation and development to be highly temporally and spatially variable around the SSI, in agreement with previous studies (Park et al.,

2010; Tynan et al., 2016). While iron is a limiting nutrient in much of the Southern Ocean (Boyd et al., 2010; de Baar et al., 1995), this is unlikely to be the case for the SSI where iron concentrations are likely to be enhanced through terrestrial iron input from the Weddell Sea and local shelf areas of the Antarctic Peninsula and South Scotia Ridge (Jiang et al., 2019; Kahru et al., 2007; Prend et al., 2019), and enhanced vertical mixing over the bathymetry of the SSI arc (Jiang et al., 2019). Instead, bloom formation is linked, at least in part, to sea ice retreat (e.g., Tynan et al., 2016) and our results suggest that the variability in the extent of sea ice and the timing of its retreat, which affect water column stability, the seasonal light climate, local nutrient fluxes and the seeding of phytoplankton blooms (see review by Deppler and Davidson, 2017, and references therein), is an important driver in the heterogeneity of blooms in this region. The spatial development of phytoplankton blooms also shows a strong relationship with the current flows, particularly in areas to the east of the islands. This indicates that mesoscale effects of enhanced nutrient supply and dispersal associated with areas of strong current flows are important in bloom development and propagation in the region. However, the spatial complexity in bloom formation, development and magnitude suggests that the exact mechanisms determining productivity and bloom development are likely to be complex and highly variable across the regions. We further note that subsurface chlorophyll maxima are a typical feature of the region (Baldry et al., 2020; Liszka et al., this issue) which have not been accounted for in our study. The observed variability emphasizes that field-based analyses of phytoplankton dynamics and carbon budgets around the SSI will require integration of seasonal and spatial variability.

4.2. Connectivity of the South Sandwich Islands system

Connectivity is a key part of the Scotia Sea ecosystem, with dispersal and retention contributing to the distribution of biota including Antarctic krill and fish (Murphy et al., 2007; Young et al., 2018). Ocean circulation connects the SSI with areas of known habitat importance in the Scotia Sea, including the Antarctic Peninsula, South Orkney Islands and South Georgia, and the Weddell Sea on relatively short timescales. Our results suggest that the southern part of the SSI arc is connected with the South Scotia Ridge and northern Weddell Sea, with the central and northern regions having broader connectivity with the Scotia Sea, including from the western Antarctic Peninsula. Transport from South Georgia can bring material to the northern end of the SSI arc. On larger scales, there is also evidence of connectivity between high latitudes in the Weddell Gyre and the SSI region. Downstream, the SSI arc is connected with other island groups, including Bouvet, Prince Edward and Marion, Crozet and Kerguelen Islands, and seamounts, with southward connection back into the eastern limb of the Weddell Gyre. These pathways and timescales of transport support the suggested role of oceanic connectivity in fish populations between the SSI and Bouvet Island (Jones et al., 2008) and also indicate that organisms for which winter sea ice is an important habitat, such as Antarctic krill, can return to sea ice covered regions downstream of the SSI and through the southward flow of the eastern limb of the Weddell Gyre, where interactions with the different advective habitats of the sea ice and ocean will affect their distribution (e.g. Thorpe et al., 2007).

Our preliminary analysis of variability in regional scale connectivity indicates that the connectivity to the SSI is spatially and temporally variable. From a study of near-surface drifters released in the northwest Weddell Sea and chlorophyll *a* distribution, Thompson and Youngs (2013) found that changes in the structure and position of the boundary currents of the Weddell Gyre and in the position of the ACC fronts affected water mass exchange between the Weddell and Scotia seas. Variability in the circulation of the ACC and Weddell Gyre is linked to their physical drivers, particularly wind forcing (see reviews by Morley et al., 2020 and Vernet et al., 2019). Armitage et al. (2018), for example, found that the speed of the Antarctic Slope Current that flows westward close to the Antarctic coast doubles in autumn, linked to changes in the

wind field and this will impact transport times from the Weddell Sea. Model analyses of particle advection from the northwestern Weddell Sea demonstrated a relationship between transport pathways into the Scotia Sea and the wind field, with greater transport across the Scotia Sea with stronger westerly winds (Renner et al., 2012), and Youngs et al. (2015) also found a relationship between wind stress curl and transport into the Scotia Sea from the Weddell Sea. Strengthening and a southward shift of the westerly wind system is one outcome of the trend in increasing SAM and this is likely to impact connectivity to the SSI by affecting the ocean currents and sea ice distribution (Meijers et al., 2012; Wang, 2013).

At the regional scale of the SSI arc, there are connections into the island arc from the south, west and north. Near-surface drifter trajectories suggest that the southern islands are strongly connected by northwards flow which is deflected to the east near the Candlemas Island group. Flow into the northern end of the island chain seems to come from a broader area, with more limited exchange with the southern areas. The local circulation is steered by the bathymetric features of the island arc. Leskov Island and the seamounts to the west of Saunders Island appear to channel flow through the passages between the islands and these locally intense, deep-reaching currents may form barriers to connectivity around the island arc and act to retain material in other locations. High resolution modelling of transport around South Georgia and the South Shetland Islands has shown the potential for locally intense flows to affect the concentration of prey around islands and it is likely that similar processes will affect the SSI ecosystem (Trathan et al., 2022; Young et al., 2014).

4.3. Ecological implications and summary comments

The complex environment of the SSI region is a major influence on primary productivity and phytoplankton and zooplankton community structure (Section 4.1; Liszka et al., this issue; Tynan et al., 2016) with the northward flow of waters from the WSC and Weddell Sea bringing more polar species into the southern areas of the SSI arc (Liszka et al., this issue; Ward et al., 2004). There is also likely to be some mixing of plankton communities as a result of transfers from the ACC in the west and north. Although the composition of zooplankton communities tends to be similar across the Scotia Sea, the relative abundance of different groups and species varies (Ward et al., 2004). Liszka et al. (this issue) found distinct mesoscale structure within the plankton community around the SSI linked to the physical oceanography. With the later retreat of sea ice in the south, plankton productivity, population and community development will tend to occur later than in lower latitude regions further north (Ward et al., 2004). The variability in ocean and ice conditions and productivity will affect the development of zooplankton populations, the dynamics of planktonic communities and food web processes, resulting in marked differences in seasonal dynamics between years and different areas.

The differing connectivities imply that planktonic communities in the SSI region can be influenced by different input regions, with varying exposure to open ocean and sea ice conditions during transport which can affect seasonal development (e.g., Fach et al., 2002; Meyer et al., 2017; Ward et al., 2004). Planktonic communities in the northern region of the SSI area are likely to be more strongly influenced by influx of planktonic organisms from the western Antarctic Peninsula and southern Scotia Sea. Those organisms are more likely to have experienced open water conditions for longer in areas of earlier ice retreat and hence better conditions for growth and development. In contrast, the most southerly areas of the SSI will be influenced by planktonic communities from the northern Weddell Sea, and are likely to be in an earlier stage of seasonal development (Ward et al., 2004). How pelagic organisms interact with ocean currents and sea ice during different stages of their life histories is crucial in determining dispersal and connectivity in the Southern Ocean (Meyer et al., 2017; Murphy et al., 2004; Thorpe et al., 2007; Young et al., 2018). Along the SSI arc, north-south differences in the distribution of lower trophic level organisms and higher trophic

level species, including fish and higher predators (Fitzcharles et al., 2021; Hart and Convey, 2018; Hollyman et al., this issue; Roberts et al., 2011), indicate spatial variability in the environmental conditions and connectivity.

Recent studies have furthered understanding of the biogeography and benthic biodiversity of the SSI arc (Downie et al., 2021; Hogg et al., 2021; Hollyman et al., this issue). There will be additional environmental and biological factors driving benthic community composition and distribution to those in the pelagic, with the degree of connectivity of populations and communities a result of mechanisms including deeper current flows and interactions with bathymetric features, life-history strategy including mode of reproduction (e.g. whether broadcast or brood spawners) and duration of pelagic larval stages, and availability of suitable settlement habitats (e.g. Roterman et al., 2016; Downie et al., 2021). At the regional scale, there is a marked distinction in the composition of the benthic community around the SSI compared to the South Orkney Islands and South Georgia (Hogg et al., 2021), potentially indicating little connectivity and exchange between these areas. The separation of the SSI and South Georgia communities is generally consistent with expectations based on the drifter and model analyses presented in our study, which illustrate relatively low likelihood of transfer across the southern ACC and SB between these regions. However, the model and drifter results indicate a high likelihood of transfer from the South Orkney Islands to the SSI region which contrasts with the lack of similarity between the benthic communities of these regions. Although we would expect a Weddell Sea influence in the southern areas of the SSI and areas to the east, the areas of the southern Scotia arc are also potential source regions for the SSI if life-history strategies permit successful transport between these regions.

The strong latitudinal variation along the SSI arc, with a greater ACC influence in the north to a more polar, Weddell Sea, influence in the south indicates that the local pelagic environments around the various SSI may be quite different. The high spatial and temporal variability is also likely to generate further differentiation between local areas. In the relatively short time series we considered, there was no signal of long term change but interannual variability and longer term trends in water mass properties, circulation and sea ice have been reported for the Scotia and Weddell seas, linked to atmospheric variation associated with Southern Hemisphere climate modes (SAM and ENSO; see reviews by Morley et al., 2020 and Vernet et al., 2019). Even without long term change, the large variability in environmental conditions, which impacts plankton distributions, productivity and zooplankton development, will generate major differences in food web structure and functioning between years and in different areas. This suggests that the development of spatial planning for conservation and management based on a view of the South Georgia SSI Marine Protected Area as a single homogeneous system may not be appropriate (cf. Hogg et al., 2021). Instead, a smaller scale approach may be required that considers the local marine system along the SSI arc. It will be important to improve knowledge of local oceanographic conditions around the islands and the local and regional oceanographic connectivity to assess the degree to which local habitats are distinct and need to be considered separately in developing plans for spatial management. Improving understanding of life history processes of organisms in the SSI and surrounding regions will be important for developing analyses of dispersal and connectivity. Combining such analyses with genetic studies provides a particularly powerful methodology for resolving levels of connectivity, which will be valuable in the complex SSI region. Such information will be critical for developing conservation and fisheries management procedures along the SSI arc, where the degree of population and genetic connectivity will need to be explicitly considered in decision making.

The SSI arc is located directly in the pathway of the eastward flowing ACC, which is deflected northwards, and influenced by currents from areas of the southern Scotia arc to the west, and the Weddell Sea to the south. The marine environment reflects, therefore, these multiple influences, generating a complex and variable system, where areas of

favourable conditions shift between years and there are marked differences in timing of seasonal development of the planktonic ecosystem and food web. Areas of more intense current flow through and around the islands may act as partial barriers to north-south exchanges or movements of organisms between the islands. At the regional scale, there are clear latitudinal differences in the environmental conditions and potential routes of connectivity transporting nutrients and organisms into the region, with stronger influences from the ACC in the north and the Weddell Gyre in the south. Improving understanding of the factors determining the structure and functioning of ecosystems across the island arc requires more information on the physical and biogeochemical environment at regional and local scales, both with seasonal data from observation systems and autonomous platforms such as Argo floats, and through the development of fine scale ocean-sea ice models that can resolve the small-scale bathymetry and processes operating in the region. The expected warming of northern waters and possible reductions of sea ice over the coming decades (Meredith et al., 2019) may result in changes in productivity, for example in timing and distribution of primary productivity (Deppler and Davidson, 2017), and habitats in northern regions becoming more favourable for sub-Antarctic species and less favourable for polar species (e.g. Cavanagh et al., 2021; Constable et al., 2014; Rintoul et al., 2018). We note, however, that regional projections of future climate change are highly uncertain at present, and robust estimates of likely outcomes will be particularly difficult to obtain in this area where the spatial and temporal scales of key physical processes are considerably smaller than presently resolved in the current suite of global climate models (Murphy et al., 2018; Johnston et al., 2022). The strong regional and local influence of sub-polar waters along the island arc is likely to be important in determining the resilience of local ecosystems. Accounting for the complexity and variability in the marine environment will be crucial in the development of conservation and fisheries management procedures for the SSI region and for ensuring, as far as possible, that ecosystem resilience is maintained as Southern Ocean environments change in the future.

Data availability

All data are publicly available through the data centres and repositories listed above and in the Acknowledgements.

Funding

This study was supported through the Natural Environment Research Council-British Antarctic Survey ALI-Science Southern Ocean Ecosystems project.

CRediT authorship contribution statement

Sally E. Thorpe: Conceptualization, Methodology, and, Writing – original draft, Writing – review & editing, Visualization. **Eugene J. Murphy:** Conceptualization, Methodology, and, Writing – original draft, Writing – review & editing.

Declaration of competing interest

The authors declare that they have no known competing financial interests or personal relationships that could have appeared to influence the work reported in this paper.

Acknowledgements

We are grateful to the investigators, programmes and services who made the datasets and software code used in this study freely available. This study has been conducted using E.U. Copernicus Marine Service and Climate Change Service Information. Sea surface temperature, sea ice concentration, GLORYS12V1 ocean reanalysis output and

chlorophyll *a* concentration data were accessed through the Copernicus Marine Service. Median sea ice extent data were provided by the National Snow and Ice Data Center. The World Ocean Atlas 2018 data were accessed from the National Oceanic and Atmospheric Administration National Centres for Environmental Information. The Global Drifter Programme data were made available through the National Oceanic and Atmospheric Administration Atlantic Oceanographic and Meteorological Laboratory. The Argo data were collected and made freely available by the International Argo Program and the national programs that contribute to it (<https://argo.ucsd.edu>). The Argo Program is part of the Global Ocean Observing System. The South Georgia and South Sandwich Islands Marine Protected Area boundary, used in Fig. 1, was downloaded from the South Georgia and South Sandwich Islands MPA GIS (https://www.sggis.gov.gs/home/sgssi_mpa) and the GEBCO gridded bathymetry was downloaded from www.gebco.net. We thank Martin Collins, Cecilia Liszka and Phil Hollyman from British Antarctic Survey and Marta Soffker from Cefas for input into the manuscript development, and Martin Biuw and two anonymous reviewers for their thoughtful comments which improved the manuscript. This paper forms a contribution to the British Antarctic Survey Ecosystems science programme.

Appendix A. Supplementary data

Supplementary data to this article can be found online at <https://doi.org/10.1016/j.dsr2.2022.105057>.

References

- Argo, 2000. Argo Float Data and Metadata from Global Data Assembly Centre (Argo GDAC). SEANOE.
- Armitage, T.W.K., Kwok, R., Thompson, A.F., Cunningham, G., 2018. Dynamic topography and sea level anomalies of the Southern Ocean: variability and teleconnections. *J. Geophys. Res. Oceans* 123, 613–630.
- Arrigo, K.R., Thomas, D.N., 2004. Large scale importance of sea ice biology in the Southern Ocean. *Antarct. Sci.* 16, 471–486.
- Artana, C., Ferrari, R., Bricaud, C., Lellouche, J.-M., Garric, G., Sennéchal, N., Lee, J.-H., Park, Y.-H., Provost, C., 2021. Twenty-five years of Mercator ocean reanalysis GLORYS12 at Drake Passage: velocity assessment and total volume transport. *Adv. Space Res.* 68, 447–466.
- Atkinson, A., Whitehouse, M.J., Priddle, J., Cripps, G.C., Ward, P., Brandon, M.A., 2001. South Georgia, Antarctica: a productive, cold water, pelagic ecosystem. *Mar. Ecol. Prog. Ser.* 216, 279–308.
- Baldry, K., Strutton, P.G., Hill, N.A., Boyd, P.W., 2020. Subsurface chlorophyll-*a* maxima in the Southern Ocean. *Front. Mar. Sci.* 7, 671.
- Borriero, I., Aumont, O., Nielsdottir, M.C., Schlitzer, R., 2014. Sedimentary and atmospheric sources of iron around South Georgia, Southern Ocean: a modelling perspective. *Biogeosciences* 11, 1981–2001.
- Borriero, I., Schlitzer, R., 2013. Distribution and recurrence of phytoplankton blooms around South Georgia, Southern Ocean. *Biogeosciences* 10, 217–231.
- Boyd, P.W., Strzepek, R., Fu, F., Hutchins, D.A., 2010. Environmental control of open-ocean phytoplankton groups: now and in the future. *Limnol. Oceanogr.* 55, 1353–1376.
- Boyer, T.P., Garcia, H.E., Locarnini, R.A., Zweng, M.M., Mishonov, A.V., Reagan, J.R., Weathers, K.A., Baranova, O.K., Paver, C.R., Seidov, D., Smolyar, I.V., 2018. World Ocean Atlas 2018. NOAA National Centers for Environmental Information.
- Brandon, M.A., Naganobu, M., Demer, D.A., Chernyshkov, P., Trathan, P.N., Thorpe, S. E., Kameda, T., Berezinskiy, O.A., Hawker, E.J., Grant, S., 2004. Physical oceanography in the Scotia Sea during the CCAMLR 2000 survey, austral summer 2000. *Deep-Sea Res. II* 51, 1301–1321.
- Cavanagh, R.D., Trathan, P.N., Hill, S.L., Melbourne-Thomas, J., Meredith, M.P., Hollyman, P., Krafft, B.A., Mc Muelbert, M., Murphy, E.J., Sommerkorn, M., Turner, J., Grant, S.M., 2021. Utilising IPCC assessments to support the ecosystem approach to fisheries management within a warming Southern Ocean. *Mar. Pol.* 131, 104589.
- Clarke, A., Griffiths, H.J., Barnes, D.K.A., Meredith, M.P., Grant, S.M., 2009. Spatial variation in seabed temperatures in the Southern Ocean: implications for benthic ecology and biogeography. *J. Geophys. Res. Oceans* 114, G03003.
- Constable, A.J., Melbourne-Thomas, J., Corney, S.P., Arrigo, K.R., Barbraud, C., Barnes, D.K.A., Bindoff, N.L., Boyd, P.W., Brandt, A., Costa, D.P., Davidson, A.T., Ducklow, H.W., Emmerson, L., Fukuchi, M., Gutt, J., Hindell, M.A., Hofmann, E.E., Hosie, G.W., Iida, T., Jacob, S., Johnston, N.M., Kawaguchi, S., Kokubun, N., Koubbi, P., Lea, M.A., Makhado, A., Massom, R.A., Meiners, K., Meredith, M.P., Murphy, E.J., Nicol, S., Reid, K., Richerson, K., Riddle, M.J., Rintoul, S.R., Smith, W. O., Southwell, C., Stark, J.S., Sumner, M., Swadling, K.M., Takahashi, K.T., Trathan, P.N., Welsford, D.C., Weimerskirch, H., Westwood, K.J., Wienecke, B.C., Wolf-Gladrow, D., Wright, S.W., Xavier, J.C., Ziegler, P., 2014. Climate change and

- Southern Ocean ecosystems I: how changes in physical habitats directly affect marine biota. *Global Change Biol.* 20, 3004–3025.
- de Baar, H.J.W., de Jong, J.T.M., Bakker, D.C.E., Loscher, B.M., Veth, C., Bathmann, U., Smetacek, V., 1995. Importance of iron for plankton blooms and carbon dioxide drawdown in the Southern Ocean. *Nature* 373, 412–415.
- Deacon, G.E.R., 1979. The Weddell Gyre. *Deep Sea Res.* 26, 981–995.
- Deppler, S.L., Davidson, A.T., 2017. Southern Ocean phytoplankton in a changing climate. *Front. Mar. Sci.* 4, 40.
- Downie, A.-L., Vieira, R.P., Hogg, O.T., Darby, C., 2021. Distribution of vulnerable marine ecosystems at the south Sandwich islands: results from the blue belt discovery expedition 99 deep-water camera surveys. *Front. Mar. Sci.* 8, 662285.
- Ducklow, H.W., Baker, K., Martinson, D.G., Quetin, L.B., Ross, R.M., Smith, R.C., Stammerjohn, S.E., Vernet, M., Fraser, W., 2007. Marine pelagic ecosystems: the West Antarctic Peninsula. *Philos. T. Roy. Soc. B* 362, 67–94.
- Fach, B.A., Hofmann, E.E., Murphy, E.J., 2002. Modeling studies of Antarctic krill *Euphausia superba* survival during transport across the Scotia Sea. *Mar. Ecol. Prog. Ser.* 231, 187–203.
- Fetterer, F., Knowles, K., Meier, W.N., Savoie, M., Windnagel, A.K., 2017. Sea Ice Index, Version 3, Updated Daily. Median Antarctic Sea Ice Extent 1981–2010. NSIDC: National Snow and Ice Data Center, Boulder, Colorado, USA.
- Fitzcharles, E., Hollyman, P.R., Goodall-Copestake, W.P., McLaine, J.S., Collins, M.A., 2021. The taxonomic identity and distribution of the eel cod *Muraenolepis* (Gadiformes: Muraenolepididae) around South Georgia and the South Sandwich Islands. *Polar Biol.* 44, 637–651.
- Froneman, P.W., Perissinotto, R., McQuaid, C.D., Laubscher, R.K., 1995. Summer distribution of net phytoplankton in the Atlantic sector of the Southern Ocean. *Polar Biol.* 15, 77–84.
- Garnesson, P., Mangin, A., Fanton d'Andon, O., Demaria, J., Bretagnon, M., 2019. The CMEMS GlobColour chlorophyll a product based on satellite observation: multi-sensor merging and flagging strategies. *Ocean Sci.* 15, 819–830.
- GEBCO Compilation Group, 2020. GEBCO2020 Grid.
- Global Monitoring and Forecasting Center, 2018. GLORYS12V1 - Global Ocean Physical Reanalysis Product. E.U. Copernicus Marine Service Information.
- Global Monitoring and Forecasting Center, 2021. Copernicus-GlobColour: Global Ocean Chlorophyll, PP and PFT from Satellite Observations: Monthly and Daily Interpolated (Reprocessed from 1997). E.U. Copernicus Marine Service Information.
- Good, S., Fiedler, E., Mao, C., Martin, M.J., Maycock, A., Reid, R., Roberts-Jones, J., Searle, T., Waters, J., While, J., Worsfold, M., 2020. The current configuration of the OSTIA system for operational production of foundation sea surface temperature and ice concentration analyses. *Rem. Sens.* 12, 720.
- Good, S.A., Embury, O., Bulgin, C.E., Mittaz, J., 2019. ESA Sea Surface Temperature Climate Change Initiative (SST_cci): Level 4 Analysis Climate Data Record, Version 2.0. Centre for Environmental Data Analysis. <https://doi.org/10.5285/aced40d7cb964f23a0fd3e85772f2d48>.
- Greene, C.A., Thirumalai, K., Kearney, K.A., Delgado, J.M., Schwanghart, W., Wolfenbarger, N.S., Thyng, K.M., Gwyther, D.E., Gardner, A.S., Blankenship, D.D., 2019. The climate data Toolbox for MATLAB. *G-cubed* 20, 3774–3781.
- Handley, J.M., Pearmain, E.J., Opper, S., Carneiro, A.P.B., Hazin, C., Phillips, R.A., Ratcliffe, N., Staniland, I.J., Clay, T.A., Hall, J., Scheffer, A., Fedak, M., Boehme, L., Putz, K., Belchier, M., Boyd, L.L., Trathan, P.N., Dias, M.P., 2020. Evaluating the effectiveness of a large multi-use MPA in protecting Key Biodiversity Areas for marine predators. *Divers. Distrib.* 26, 715–729.
- Hart, T., Convey, P., 2018. The South Sandwich Islands – a community of meta-populations across all trophic levels. *Biodiversity* 19, 20–33.
- Heywood, K.J., Naveira Garabato, A.C., Stevens, D.P., Muench, R.D., 2004. On the fate of the Antarctic slope front and the origin of the Weddell front. *J. Geophys. Res. Oceans* 109, C06021.
- Hinz, D.J., Nielsdottir, M.C., Korb, R.E., Whitehouse, M.J., Poulton, A.J., Moore, C.M., Achterberg, E.P., Bibby, T.S., 2012. Responses of microplankton community structure to iron addition in the Scotia Sea. *Deep-Sea Res.* II 59, 36–46.
- Hodson, A., Nowak, A., Sabacka, M., Jungblut, A., Navarro, F., Pearce, D., Avila-Jimenez, M.L., Convey, P., Vieira, G., 2017. Climatically sensitive transfer of iron to maritime Antarctic ecosystems by surface runoff. *Nat. Commun.* 8, 14499.
- Hofmann, E.E., Murphy, E.J., 2004. Advection, krill, and Antarctic marine ecosystems. *Antarct. Sci.* 16, 487–499.
- Hogg, O.T., Downie, A.L., Vieira, R., Darby, C., 2021. Macrobenthic assessment of the South Sandwich Islands reveals a biogeographically distinct polar archipelago. *Front. Mar. Sci.* 8, 650241.
- Hollyman, P.R., Soeffker, M., Roberts, J., Hogg, O.T., Laptikhovskiy, V.V., Queirós, J.P., Darby, C., Belchier, M., Collins, M.A., This Issue. Bioregionalization of the South Sandwich Islands through Community Analysis of Bathyal Fish and Invertebrate Assemblages Using Fishery-Derived Data. *Deep-Sea Res.* II, (in revision). <https://doi.org/10.1016/j.dsr2.2022.105054>.
- Hunt, G.L., Drinkwater, K.F., Arrigo, K., Berge, J., Daly, K.L., Danielson, S., Daase, M., Hop, H., Isla, E., Karnovsky, N., Laidre, K., Mueter, F.J., Murphy, E.J., Renaud, P.E., Smith, W.O., Trathan, P., Turner, J., Wolf-Gladrow, D., 2016. Advection in polar and sub-polar environments: impacts on high latitude marine ecosystems. *Prog. Oceanogr.* 149, 40–81.
- Jiang, M., Measures, C.I., Barbeau, K.A., Charette, M.A., Gille, S.T., Hatta, M., Kahru, M., Mitchell, B.G., Garabato, A.C.N., Reiss, C., Selph, K., Zhou, M., 2019. Fe sources and transport from the Antarctic Peninsula shelf to the southern Scotia Sea. *Deep-Sea Res.* I 150, 103060.
- Johnston, N.M., Murphy, E.J., Atkinson, A.A., Constable, A.J., Cotté, C.S., Cox, M., Daly, K.L., Driscoll, R., Flores, H., Halfler, S., Henschke, N., Hill, S.L., Höfer, J., Hunt, B.P.V., Kawaguchi, S., Lindsay, D., Liszka, C., Loeb, V., Manno, C., Meyer, B., Pakhomov, E.A., Pinkerton, M.H., Reiss, C.S., Richerson, K., Smith Jr., W.O., Steinberg, D.K., Swadling, K.M., Tarling, G.A., Thorpe, S.E., Veytia, D., Ward, P., Weldrick, C.K., Yang, G., 2022. Status, change and futures of zooplankton in the Southern Ocean. *Front. Ecol. Evol.* 9 <https://doi.org/10.3389/fevo.2021.624692>.
- Jones, C.D., Anderson, M.E., Balushkin, A.V., Duhamel, G., Eakin, R.R., Eastman, J.T., Kuhn, K.L., Lecointre, G., Near, T.J., North, A.W., Stein, D.L., Vacchi, M., Detrich, H.W., 2008. Diversity, relative abundance, new locality records and population structure of Antarctic demersal fishes from the northern Scotia Arc islands and Bouvetoya. *Polar Biol.* 31, 1481–1497.
- Kahru, M., Mitchell, B.G., Gille, S.T., Hewes, C.D., Holm-Hansen, O., 2007. Eddies enhance biological production in the weddell-scotia confluence of the Southern Ocean. *Geophys. Res. Lett.* 34, L14603.
- Kim, Y.S., Orsi, A.H., 2014. On the variability of Antarctic circumpolar current fronts inferred from 1992–2011 altimetry. *J. Phys. Oceanogr.* 44, 3054–3071.
- Korb, R.E., Whitehouse, M.J., Atkinson, A., Thorpe, S.E., 2008. Magnitude and maintenance of the phytoplankton bloom at South Georgia: a naturally iron-replete environment. *Mar. Ecol. Prog. Ser.* 368, 75–91.
- Korb, R.E., Whitehouse, M.J., Ward, P., Gordon, M., Venables, H.J., Poulton, A.J., 2012. Regional and seasonal differences in microplankton biomass, productivity, and structure across the Scotia Sea: implications for the export of biogenic carbon. *Deep-Sea Res.* II 59, 67–77.
- Lavergne, T., Sørensen, A.M., Kern, S., Tonboe, R., Notz, D., Aaboe, S., Bell, L., Dybkjær, G., Eastwood, S., Gabarro, C., Heygster, G., Killie, M.A., Brandt Kreiner, M., Lavelle, J., Saldo, R., Sandven, S., Pedersen, L.T., 2019. Version 2 of the EUMETSAT OSI SAF and ESA CCI sea-ice concentration climate data records. *Cryosphere* 13, 49–78.
- Leat, P.T., Fretwell, P.T., Tate, A.J., Larter, R.D., Martin, T.J., Smellie, J.L., Jokat, W., Bohrmann, G., 2014. Bathymetry and Geological Setting of the South Sandwich Islands Volcanic Arc (Various Scales), BAS GEOMAP 2 Series. British Antarctic Survey, Cambridge. Sheet 6.
- Leat, P.T., Fretwell, P.T., Tate, A.J., Larter, R.D., Martin, T.J., Smellie, J.L., Jokat, W., Bohrmann, G., 2016. Bathymetry and geological setting of the South Sandwich Islands volcanic arc. *Antarct. Sci.* 28, 293–303.
- Liszka, C.M., Thorpe, S.E., Wootton, M., Fielding, S., Murphy, E., Tarling, G., This Issue. Plankton and Nekton Community Structure in the Vicinity of the South Sandwich Islands (Southern Ocean) and the Influence of Environmental Factors Deep-Sea Res. II. (In revision).
- Locarnini, R.A., Mishonov, A.V., Baranova, O.K., Boyer, T.P., Zweng, M.M., Garcia, H.E., Reagan, J.R., Seidov, D., Weathers, K., Paver, C.R., Smolyar, I., 2019. World Ocean Atlas 2018, Volume 1: Temperature. In: Mishonov, A.T.E. (Ed.), NOAA Atlas NESDIS, p. 52.
- Locarnini, R.A., Whitworth III, T., Nowlin Jr., W.D., 1993. The importance of the Scotia Sea on the outflow of Weddell sea deep water. *J. Mar. Res.* 51, 135–153.
- Lumpkin, R., Centurioni, L., 2019. NOAA Global Drifter Program Quality-Controlled 6-hour Interpolated Data from Ocean Surface Drifting Buoys. NOAA National Centers for Environmental Information [September 2020 update].
- Lumpkin, R., Özgökmen, T., Centurioni, L., 2017. Advances in the application of surface drifters. *Ann. Rev. Mar. Sci.* 9, 59–81.
- Lumpkin, R., Pazos, M., 2007. Measuring surface currents with Surface Velocity Program drifters: the instrument, its data, and some recent results. In: Kirwan, J.A.D., Griffa, A., Mariano, A.J., Rossby, H.T., Özgökmen, T. (Eds.), Lagrangian Analysis and Prediction of Coastal and Ocean Dynamics. Cambridge University Press, Cambridge, pp. 39–67.
- Meijers, A.J.S., Shuckburgh, E., Bruneau, N., Sallee, J.-B., Bracegirdle, T.J., Wang, Z., 2012. Representation of the Antarctic Circumpolar Current in the CMIP5 climate models and future changes under warming scenarios. *J. Geophys. Res. Oceans* 117, C12008.
- Merchant, C.J., Embury, O., Bulgin, C.E., Block, T., Corlett, G.K., Fiedler, E., Good, S.A., Mittaz, J., Rayner, N.A., Berry, D., Eastwood, S., Taylor, M., Tsushima, Y., Waterfall, A., Wilson, R., Donlon, C., 2019. Satellite-based time-series of sea-surface temperature since 1981 for climate applications. *Sci. Data* 6, 223.
- Meredith, M.P., Brandon, M.A., Murphy, E.J., Trathan, P.N., Thorpe, S.E., Bone, D.G., Chernyshkov, P.P., Sushin, V.A., 2005. Variability in hydrographic conditions to the east and northwest of South Georgia, 1996–2001. *J. Mar. Syst.* 53, 143–167.
- Meredith, M.P., Meijers, A.S., Naveira Garabato, A.C., Brown, P.J., Venables, H.J., Abrahamson, E.P., Jullion, L., Messias, M.-J., 2015. Circulation, retention, and mixing of waters within the Weddell-Scotia Confluence, Southern Ocean: the role of stratified Taylor columns. *J. Geophys. Res. Oceans* 120, 547–562.
- Meredith, M., Sommerkorn, M., Cassotta, S., Derksen, C., Ekaykin, A., Hollowed, A., Kofinas, G., Mackintosh, A., Melbourne-Thomas, J., Muelbert, M.M.C., Ottersen, G., Pritchard, H., Schuur, E.A.G., 2019. Polar regions. In: Pörtner, H.-O., Roberts, D.C., Masson-Delmotte, V., Zhai, P., Tignor, M., Poloczanska, E., Mintenbeck, K., Alegría, A., Nicolai, M., Okem, A., Petzold, J., Rama, B., Weyer, N.M. (Eds.), IPCC Special Report on the Ocean and Cryosphere in a Changing Climate.
- Meyer, B., Freier, U., Grimm, V., Groeneveld, J., Hunt, B.P.V., Kerwath, S., Kin, R., Klaas, C., Pakhomov, E., Meiners, K.M., Melbourne-Thomas, J., Murphy, E.J., Thorpe, S.E., Stammerjohn, S., Wolf-Gladrow, D., Auerswald, L., Gotz, A., Halbach, L., Jarman, S., Kawaguchi, S., Krumpen, T., Nehrke, G., Ricker, R., Sunner, M., Teschke, M., Trebilco, R., Yilmaz, N.I., 2017. The winter pack-ice zone provides a sheltered but food-poor habitat for larval Antarctic krill. *Nature Ecol. Evol.* 1, 1853–1861.
- Morley, S.A., Abele, D., Barnes, D.K.A., Cárdenas, C.A., Cotté, C., Gutt, J., Henley, S.F., Höfer, J., Hughes, K.A., Martin, S.M., Moffat, C., Raphael, M., Stammerjohn, S.E., Suckling, C.C., Tulloch, V.J.D., Waller, C.L., Constable, A.J., 2020. Global drivers on Southern Ocean ecosystems: changing physical environments and anthropogenic pressures in an Earth system. *Front. Mar. Sci.* 7, 547188.

- Murphy, E.J., Cavanagh, R.D., Drinkwater, K.F., Grant, S.M., Heymans, J.J., Hofmann, E., Hunt, G.L., Johnston, N.M., 2016. Understanding the structure and functioning of polar pelagic ecosystems to predict the impacts of change. *P. Roy. Soc. B-Biol. Sci.* 283, 20161646.
- Murphy, E.J., Clarke, A., Abram, N.J., Turner, J., 2014. Variability of sea-ice in the northern Weddell Sea during the 20th century. *J. Geophys. Res. Oceans* 119, 4549–4572.
- Murphy, E., Johnston, N., Corney, S., Reid, K., 2018. Integrating climate and ecosystem dynamics in the Southern Ocean (ICED) programme: report of the ICED-CCAMLR projections workshop, 5-7 Apr 2018. SC-CAMLRXXXVII/BG/16. In: SC-CAMLR-XXXVII. Hobart. CCAMLR, Tasmania.
- Murphy, E.J., Thorpe, S.E., Watkins, J.L., Hewitt, R., 2004. Modeling the krill transport pathways in the Scotia Sea: spatial and environmental connections generating the seasonal distribution of krill. *Deep-Sea Res. II* 51, 1435–1456.
- Murphy, E.J., Watkins, J.L., Trathan, P.N., Reid, K., Meredith, M.P., Thorpe, S.E., Johnston, N.M., Clarke, A., Tarling, G.A., Collins, M.A., Forcada, J., Shreeve, R.S., Atkinson, A., Korb, R., Whitehouse, M.J., Ward, P., Rodhouse, P.G., Enderlein, P., Hirst, A.G., Martin, A.R., Hill, S.L., Staniland, I.J., Pond, D.W., Briggs, D.R., Cunningham, N.J., Fleming, A.H., 2007. Spatial and temporal operation of the Scotia Sea ecosystem: a review of large-scale links in a krill centred food web. *Philos. T. Roy. Soc. B* 362, 113–148.
- Naveira Garabato, A.C., Heywood, K.J., Stevens, D.P., 2002. Modification and pathways of Southern Ocean deep waters in the Scotia Sea. *Deep Sea Res. I* 49, 681–705.
- Nielsdotir, M.C., Bibby, T.S., Moore, C.M., Hinz, D.J., Sanders, R., Whitehouse, M., Korb, R., Achterberg, E.P., 2012. Seasonal and spatial dynamics of iron availability in the Scotia Sea. *Mar. Chem.* 130, 62–72.
- Orsi, A.H., Nowlin Jr., W.D., Whitworth III, T., 1993. On the circulation and stratification of the Weddell Gyre. *Deep-Sea Res.* 40, 169–203.
- Orsi, A.H., Whitworth, T., Nowlin, W.D., 1995. On the meridional extent and fronts of the Antarctic Circumpolar Current. *Deep Sea Res. I* 42, 641–673.
- Park, J., Oh, I.S., Kim, H.C., Yoo, S., 2010. Variability of SeaWiFs chlorophyll-a in the southwest Atlantic sector of the Southern Ocean: strong topographic effects and weak seasonality. *Deep-Sea Res. I* 57, 604–620.
- Park, Y.-H., Charriaud, E., Craneguy, P., Kartavtseff, A., 2001. Fronts, transport, and Weddell Gyre at 30°E between Africa and Antarctica. *J. Geophys. Res. Oceans* 106, 2857–2879.
- Park, Y.-H., Durand, I., 2019. Altimetry-derived Antarctic Circumpolar Current Fronts. SEANO.
- Park, Y.-H., Park, T., Kim, T.-W., Lee, S.-H., Hong, C.-S., Lee, J.-H., Rio, M.-H., Pujol, M.-I., Ballarotta, M., Durand, I., Provost, C., 2019. Observations of the Antarctic circumpolar current over the udintsev fracture zone, the narrowest choke point in the Southern Ocean. *J. Geophys. Res. Oceans* 124, 4511–4528.
- Pawlowicz, R., 2020. M Map: A Mapping Package for MATLAB version 1.4m.
- Perissinotto, R., Laubscher, R.K., McQuaid, C.D., 1992. Marine productivity enhancement around Bouvet and the south Sandwich islands (Southern Ocean). *Mar. Ecol. Prog. Ser.* 88, 41–53.
- Prend, C.J., Gille, S.T., Talley, L.D., Mitchell, B.G., Rosso, I., Mazloff, M.R., 2019. Physical drivers of phytoplankton bloom initiation in the Southern Ocean's Scotia Sea. *J. Geophys. Res. Oceans* 124, 5811–5826.
- Reeve, K.A., Boebel, O., Strass, V., Kanzow, T., Gerdes, R., 2019. Horizontal circulation and volume transports in the Weddell Gyre derived from Argo float data. *Prog. Oceanogr.* 175, 263–283.
- Renner, A.H.H., Thorpe, S.E., Heywood, K.J., Murphy, E.J., Watkins, J.L., Meredith, M.P., 2012. Advective pathways near the tip of the Antarctic Peninsula: trends, variability and ecosystem implications. *Deep-Sea Res. I* 63, 91–101.
- Rintoul, S.R., Chown, S.L., DeConto, R.M., England, M.H., Fricker, H.A., Masson-Delmotte, V., Naish, T.R., Siebert, M.J., Xavier, J.C., 2018. Choosing the future of Antarctica. *Nature* 558, 233–241.
- Roberts, J., Xavier, J.C., Agnew, D.J., 2011. The diet of toothfish species *Dissostichus eleginoides* and *Dissostichus mawsoni* with overlapping distributions. *J. Fish. Biol.* 79, 138–154.
- Robinson, J., New, A.L., Popova, E.E., Srokosz, M.A., Yool, A., 2017. Far-field connectivity of the UK's four largest marine protected areas: four of a kind? *Earth's Future* 5, 475–494.
- Rogers, A.D., Yesson, C., Gravestock, P., 2015. A biophysical and economic profile of South Georgia and the South Sandwich Islands as potential large-scale Antarctic protected areas. In: Curry, B.E. (Ed.), *Advances in Marine Biology*, 70, pp. 1–286.
- Roterman, C.N., Copley, J.T., Linse, K.T., Tyler, P.A., Rogers, A.D., 2016. Connectivity in the cold: the comparative population genetics of vent-endemic fauna in the Scotia Sea, Southern Ocean. *Mol. Ecol.* 25, 1073–1088.
- Saba, G.K., Fraser, W.R., Saba, V.S., Iannuzzi, R.A., Coleman, K.E., Doney, S.C., Ducklow, H.W., Martinson, D.G., Miles, T.N., Patterson-Fraser, D.L., Stammerjohn, S.E., Steinberg, D.K., Schofield, O.M., 2014. Winter and spring controls on the summer food web of the coastal West Antarctic Peninsula. *Nat. Commun.* 5, 4318.
- Sergi, S., Baudena, A., Cotte, C., Ardyna, M., Blain, S., d'Ovidio, F., 2020. Interaction of the Antarctic Circumpolar Current with seamounts fuels moderate blooms but vast foraging grounds for multiple marine predators. *Front. Mar. Sci.* 7, 416.
- Smith, W.O., Ainley, D.G., Cattaneo-Vietti, R., 2007. Trophic interactions within the Ross Sea continental shelf ecosystem. *Philos. T. Roy. Soc. B* 362, 95–111.
- Sokolov, S., Rintoul, S.R., 2009. Circumpolar structure and distribution of the Antarctic Circumpolar Current fronts: 1. Mean circumpolar paths. *J. Geophys. Res. Oceans* 114, C11018.
- Stammerjohn, S.E., Martinson, D.G., Smith, R.C., Yuan, X., Rind, D., 2008. Trends in Antarctic annual sea ice retreat and advance and their relation to El Niño–southern oscillation and southern Annular mode variability. *J. Geophys. Res. Oceans* 113, C03S90.
- Stroeve, J.C., Jenouvrier, S., Campbell, G.G., Barbraud, C., Delord, K., 2016. Mapping and assessing variability in the Antarctic marginal ice zone, pack ice and coastal polynyas in two sea ice algorithms with implications on breeding success of snow petrels. *Cryosphere* 10, 1823–1843.
- Thompson, A.F., Youngs, M.K., 2013. Surface exchange between the Weddell and Scotia seas. *Geophys. Res. Lett.* 40, 5920–5925.
- Thorpe, S.E., Murphy, E.J., Watkins, J.L., 2007. Circumpolar connections between Antarctic krill (*Euphausia superba* Dana) populations: investigating the roles of ocean and sea ice transport. *Deep-Sea Res. I* 54, 792–810.
- Thyng, K.M., Greene, C.A., Hetland, R.D., Zimmerle, H.M., DiMarco, S.F., 2016. True colors of oceanography: Guidelines for effective and accurate colormap selection. *Oceanography* 29, 9–13.
- Trathan, P.N., Collins, M.A., Grant, S.M., Belchier, M., Barnes, D.K.A., Brown, J., Staniland, I.J., 2014. The South Georgia and the South Sandwich Islands MPA: protecting a biodiverse oceanic island chain situated in the flow of the Antarctic Circumpolar Current. In: Johnson, M.L., Sandell, J. (Eds.), *Marine Managed Areas and Fisheries*, vol. 69. *Adv. Mar. Biol.*, pp. 15–78.
- Trathan, P.N., Warwick-Evans, V., Young, E.F., Friedlaender, A., Kim, J.H., Kokubun, N., 2022. The ecosystem approach to management of the Antarctic krill fishery - the 'devils are in the detail' at small spatial and temporal scales. *J. Mar. Syst.* 225, 103598.
- Tynan, E., Clarke, J.S., Humphreys, M.P., Ribas-Ribas, M., Esposito, M., Rerolle, V.M.C., Schlosser, C., Thorpe, S.E., Tyrrell, T., Achterberg, E.P., 2016. Physical and biogeochemical controls on the variability in surface pH and calcium carbonate saturation states in the Atlantic sectors of the Arctic and Southern Oceans. *Deep-Sea Res. II* 127, 7–27.
- Venables, H., Meredith, M.P., Atkinson, A., Ward, P., 2012. Fronts and habitat zones in the Scotia Sea. *Deep-Sea Res. II* 59–60, 14–24.
- Vernet, M., Geibert, W., Hoppema, M., Brown, P.J., Haas, C., Hellmer, H.H., Jokat, W., Jullion, L., Mazloff, M., Bakker, D.C.E., Brearley, J.A., Croot, P., Hattermann, T., Hauck, J., Hillenbrand, C.-D., Hoppe, C.J.M., Huhn, O., Koch, B.P., Lechtenfeld, O.J., Meredith, M.P., Naveira Garabato, A.C., Nöthig, E.-M., Peeken, I., Rutgers van der Loeff, M.M., Schmidt, S., Schröder, M., Strass, V.H., Torres-Valdés, S., Verdy, A., 2019. The Weddell Gyre, Southern Ocean: present knowledge and future challenges. *Rev. Geophys.* 57, 623–708.
- Wang, Z., 2013. On the response of Southern Hemisphere subpolar gyres to climate change in coupled climate models. *J. Geophys. Res. Oceans* 118, 1070–1086.
- Ward, P., Atkinson, A., Tarling, G., 2012a. Mesozooplankton community structure and variability in the Scotia Sea: a seasonal comparison. *Deep-Sea Res. II* 59, 78–92.
- Ward, P., Atkinson, A., Venables, H.J., Tarling, G.A., Whitehouse, M.J., Fielding, S., Collins, M.A., Korb, R., Black, A., Stowasser, G., Schmidt, K., Thorpe, S.E., Enderlein, P., 2012b. Food web structure and bioregions in the Scotia Sea: a seasonal synthesis. *Deep-Sea Res. II* 59, 253–266.
- Ward, P., Grant, S., Brandon, M., Siegel, V., Sushin, V., Loeb, V., Griffiths, H., 2004. Mesozooplankton community structure in the Scotia Sea during the CCAMLR 2000 survey: January-February 2000. *Deep-Sea Res. II* 51, 1351–1367.
- Whitehouse, M.J., Atkinson, A., Korb, R.E., Venables, H.J., Pond, D.W., Gordon, M., 2012. Substantial primary production in the land-remote region of the central and northern Scotia Sea. *Deep-Sea Res. II* 59, 47–56.
- Whitworth, T., Nowlin, W.D., Orsi, A.H., Locarnini, R.A., Smith, S.G., 1994. Weddell sea shelf water in the Bransfield Strait and weddell-scotia confluence. *Deep Sea Res. I* 41, 629–641.
- Young, E.F., Thorpe, S.E., Banglawala, N., Murphy, E.J., 2014. Variability in transport pathways on and around the South Georgia shelf, Southern Ocean: implications for recruitment and retention. *J. Geophys. Res. Oceans* 119, 241–252.
- Young, E.F., Tysklind, N., Meredith, M.P., de Bruyn, M., Belchier, M., Murphy, E.J., Carvalho, G.R., 2018. Stepping stones to isolation: impacts of a changing climate on the connectivity of fragmented fish populations. *Evol. Appl.* 11, 978–994.
- Youngs, M.K., Thompson, A.F., Flexas, M.M., Heywood, K.J., 2015. Weddell Sea export pathways from surface drifters. *J. Phys. Oceanogr.* 45, 1068–1085.
- Zweng, M.M., Reagan, J.R., Seidov, D., Boyer, T.P., Locarnini, R.A., Garcia, H.E., Mishonov, A.V., Baranova, O.K., Weathers, K., Paver, C.R., Smolyar, I., 2019. *World Ocean Atlas 2018, Volume 2: Salinity*. In: Mishonov, A.T.E. (Ed.), *NOAA Atlas NESDIS*, p. 50.